doi:10.26443/seismica.v2i4.1477

No evidence for an active margin-spanning megasplay fault at the Cascadia Subduction Zone

Madeleine C. Lucas *[1], **Anna M. Ledeczi** [1], **Harold J. Tobin** [1], **Suzanne. M. Carbotte** [2], **Janet T. Watt** [3], **Shuoshuo Han** [4], **Brian Boston** [5], **Danqi Jiang** [4]

[1]Department of Earth & Space Sciences, University of Washington, Seattle, WA, [2]Lamont Doherty Earth Observatory, Columbia University, New York City, NY, [3]U.S. Geological Survey, Pacific Coastal and Marine Science Center, Santa Cruz, CA, [4]Institute for Geophysics, University of Texas at Austin, Austin, TX, [5]Department of Geosciences, Auburn University, Auburn, AL

Author contributions: *Conceptualization*: M. C. Lucas, H. J. Tobin, J. T. Watt. *Methodology*: M. C. Lucas. *Investigation*: M. C. Lucas, A. M. Ledeczi. *Validation*: A. M. Ledeczi, H. J. Tobin, S. M. Carbotte, J. T. Watt, S. Han, B. Boston, D. Jiang. *Supervision*: H. J. Tobin, S. M. Carbotte, J. T. Watt, S. Han, B. Boston. *Writing – original draft*: M. C. Lucas. *Writing – review & editing*: M. C. Lucas, A. M. Ledeczi, H. J. Tobin, S. M. Carbotte, J. T. Watt, S. Han, B. Boston, D. Jiang. *Funding Acquisition*: H. J. Tobin, S. M. Carbotte, S. Han, B. Boston.

Abstract It has been previously proposed that a megasplay fault within the Cascadia accretionary wedge, spanning from offshore Vancouver Island to Oregon, has the potential to slip during a future Cascadia subduction zone earthquake. This hypothetical fault has major implications for tsunami size and arrival times and is included in disaster-planning scenarios currently in use in the region. This hypothesis is evaluated in this study using CASIE21 deep-penetrating and U.S. Geological Survey high-resolution seismic reflection profiles. We map changes in wedge structural style and seismic character to identify the inner-outer wedge transition zone where a megasplay fault has been previously hypothesized to exist and evaluate evidence for active faulting within this zone. Our results indicate that there is not an active, through-going megasplay fault in Cascadia, but instead, the structure and activity of faulting at the inner-outer wedge transition zone is highly variable and segmented along strike, consistent with the segmentation of other physical and mechanical properties in Cascadia. Wedge sedimentation, plate dip, and subducting topography are proposed to play a major role in controlling megasplay fault development and evolution. Incorporating updated megasplay fault location, geometry, and activity into modeling of Cascadia earthquakes and tsunamis could help better constrain associated hazards.

Production Editor:
Christie Rowe
Alice Agnes Gabriel
Handling Editor:
Isabel Hong
Christie Rowe
Copy & Layout Editor:
Hannah F. Mark

Signed reviewer(s):
Ryu Arai

Received:
September 30, 2024
Accepted:
April 15, 2025
Published:
May 6, 2025

1 Introduction

Slip on splay faults during Cascadia megathrust earthquakes has the potential to significantly increase vertical seafloor displacement and tsunami size, posing an enhanced tsunami hazard to coastal communities in the Pacific Northwest (Geist and Yoshioka, 1996; Priest et al., 2009; Witter et al., 2013; Gao et al., 2018; Sypus, 2019; Lotto et al., 2018). However, little is known about which splay faults in the Cascadia accretionary wedge are currently active and have the potential to slip in the next megathrust earthquake (e.g., Wang and Tréhu, 2016). Stress barriers in the accretionary wedge created by major contrasts in wedge lithology and strength can promote splay fault rupture (Byrne et al., 1993; Wendt et al., 2009). Splay fault rupture at stress barriers has been observed in recent large megathrust earthquakes, including the 1964 Alaska Mw 9.2 (Plafker, 1969; Liberty et al., 2013; Haeussler et al., 2015), 1944 Tonankai Mw 8.2 (Park et al., 2002; Moore et al., 2007), and 2004 Sumatra Mw 9.2 (Sibuet et al., 2007), and is considered to have significantly contributed to tsunami generation (Plafker, 1965; Cummins and Kaneda, 2000; Baba and Cummins, 2005).

It has been previously hypothesized that there is an active megasplay fault system in Cascadia spanning the margin from Vancouver Island to Oregon that is coincident with a major stress barrier in the accretionary wedge where there is a change in wedge lithology and strength (e.g., Witter et al., 2013; Watt and Brothers, 2020) (Fig. 1). A megasplay fault, as defined by previous work, is a persistent, large, out-of-sequence thrust fault or fault system within the accretionary wedge of a subduction zone that merges with the main megathrust fault at depth while also branching up to the seafloor (e.g., Tobin and Kinoshita, 2006; Moore et al., 2007). Analysis of early seismic imaging of the Cascadia subduction zone identified out-of-sequence, megasplay-style faults in the accretionary wedge branching from the megathrust fault up to the seafloor, cutting across the multiple sedimentary units that make up the Cascadia accretionary wedge and focused at a major lithologic boundary in the wedge (Snavely, 1987; Goldfinger, 1994; Goldfinger et al., 1997). The age of offshore accretionary wedge complexes was previously inferred from bedrock outcrops on the western Olympic Peninsula and industry boreholes on the continental shelf (Palmer and Lingley, 1989; McNeill et al., 1997). Watt and Brothers (2020) furthered analysis of offshore wedge lithology and faulting by inferring the boundary between the older, stronger Miocene

*Corresponding author: mlucas12@uw.edu

wedge and younger, weaker Pleistocene accretionary wedge (i.e., dynamic backstop; Fig. 1) based on morphologic breaks in wedge surface slope interpreted from seafloor bathymetry. They found that the dynamic backstop exists along the hypothesized megasplay fault from Witter et al. (2013). However, they specify that this fault at the dynamic backstop requires further evaluation with modern multibeam bathymetry and high-resolution seismic reflection imaging at different scales to resolve how deep fault structure connects to near-surface fault deformation, indicating megasplay fault activity within the late Pleistocene to Holocene periods.

Studies modeling megathrust earthquakes and tsunamis at the Cascadia subduction zone often include a scenario with margin-wide rupture on this hypothetical megasplay fault (Fig. 1) (Priest et al., 2009; Witter et al., 2013; Gao et al., 2018; Sypus, 2019; Lotto et al., 2018). In these studies, scenarios including megasplay fault rupture exhibit significantly higher tsunami wave heights and run-ups and shorter tsunami arrival times compared to scenarios modeling only megathrust fault rupture. The hypothesized megasplay fault is generalized as a continuous along-strike, seaward-verging thrust fault structure dipping landward at about 30° and merging with the megathrust at depths less than ~20 km (Priest et al., 2009; Witter et al., 2013; Gao et al., 2018). Although this megasplay fault geometry is the most commonly used, other geometries and locations for this fault have been tested (Gao et al., 2018; Aslam et al., 2021). Due to relatively poor data quality and limited spatial coverage of legacy geophysical experiments, many of these studies emphasize that the geometry, location, and activity of the hypothesized fault is not conclusive and further structural analysis of this fault is needed to determine its existence and likelihood of rupture in future earthquakes. Despite this, the megasplay fault scenario as described has been consistently included in modern hazard assessments due to the potential for this fault to significantly contribute to tsunamigenesis in a future Cascadia earthquake (Wang and Tréhu, 2016), as demonstrated at other subduction zones.

In this study, we use 2D seismic reflection data from the CAscadia Seismic Imaging Experiment 2021 (CASIE21) (Carbotte et al., 2021) to evaluate the hypothesis for a megasplay fault at Cascadia. Using CASIE21 seismic profiles, we characterize the nature of the transition between the inner and outer domains of the Cascadia accretionary wedge. Our analysis focuses on differences in structural style and seismic character between the inner and outer wedge domains, defining the spatial extent of the "inner-outer wedge transition zone" (IOWTZ) in Cascadia. Then, we evaluate evidence for the presence of a megasplay fault structure at the IOWTZ. Evidence for an active, margin-spanning megasplay fault system is investigated by linking observations of fault structure, activity, and continuity along strike at or near the IOWTZ.

2 Data and Methods

2.1 Terminology

There is a clear agreement among previous studies that a major structural boundary exists within the Cascadia accretionary wedge between older and younger wedge terranes offshore the northern region (Vancouver Island, Washington, northern Oregon) of the Cascadia margin (Silver, 1972; Mann and Snavely, 1984; Davis and Hyndman, 1989; Hyndman et al., 1990; Flueh et al., 1998; McNeill et al., 2000; Adam et al., 2004; Webb, 2017; Watt and Brothers, 2020; Snavely, 1987). Because terminology used to describe this boundary is ambiguous, we define the terms and criteria used in this study. We choose to not use the term "backstop" because it implies information about wedge strength and deformation. For example, the term "dynamic backstop" has been used to describe an actively deforming backstop where older accreted materials are still deforming as new material is accreted to the wedge (Kopp and Kukowski, 2003; Watt and Brothers, 2020). Conversely, the term "static backstop" has been used to describe a backstop that is no longer actively deforming between the accretionary wedge and crystalline, continental backstops (Silver et al., 1985; Byrne et al., 1993; Kopp and Kukowski, 2003; Watt and Brothers, 2020). Instead, we use the term "inner wedge" to describe the older (inferred Miocene) accretionary wedge complex; and the term "outer wedge" to describe the younger (inferred Pleistocene) accretionary wedge complex. Our use of these terms deviates from morphological uses of the terms in which the boundary between the inner and outer wedge is defined by the outer arc high. This terminology allows for our analysis of wedge structure to be independent from surface morphology and active deformation.

2.2 Geophysical Datasets

To characterize the transition between the inner and outer wedge domains of the Cascadia accretionary wedge, we use ultra-long offset seismic reflection images from CASIE21, which capture subsurface structure to depths greater than 10 km. CASIE21 utilized the *R/V Marcus G. Langseth* to complete the first modern, regional-scale seismic reflection imaging survey of the offshore Cascadia subduction zone (Carbotte et al., 2021, 2023). In the CASIE21 survey, we collected 2-D multi-channel seismic (MCS) reflection and multibeam bathymetric data along 18 primary dip lines, 7 strike lines, and several turning lines, from Vancouver Island to southern Oregon (Fig. 1). Dip lines are interpreted in this study because they provide a cross-sectional view of accretionary wedge structure. All seismic profiles in this study are presented with the seaward direction (west) to the left and the landward direction (east) on the right. Data acquisition was carried out with a 12-15 km-long streamer and a 36-airgun array with a maximum volume of 6600 cubic inches. CASIE21 MCS data were processed by ION Geophysical to produce prestack depth migrated (PSDM) MCS reflection profiles. Processed seismic lines are available on the Marine

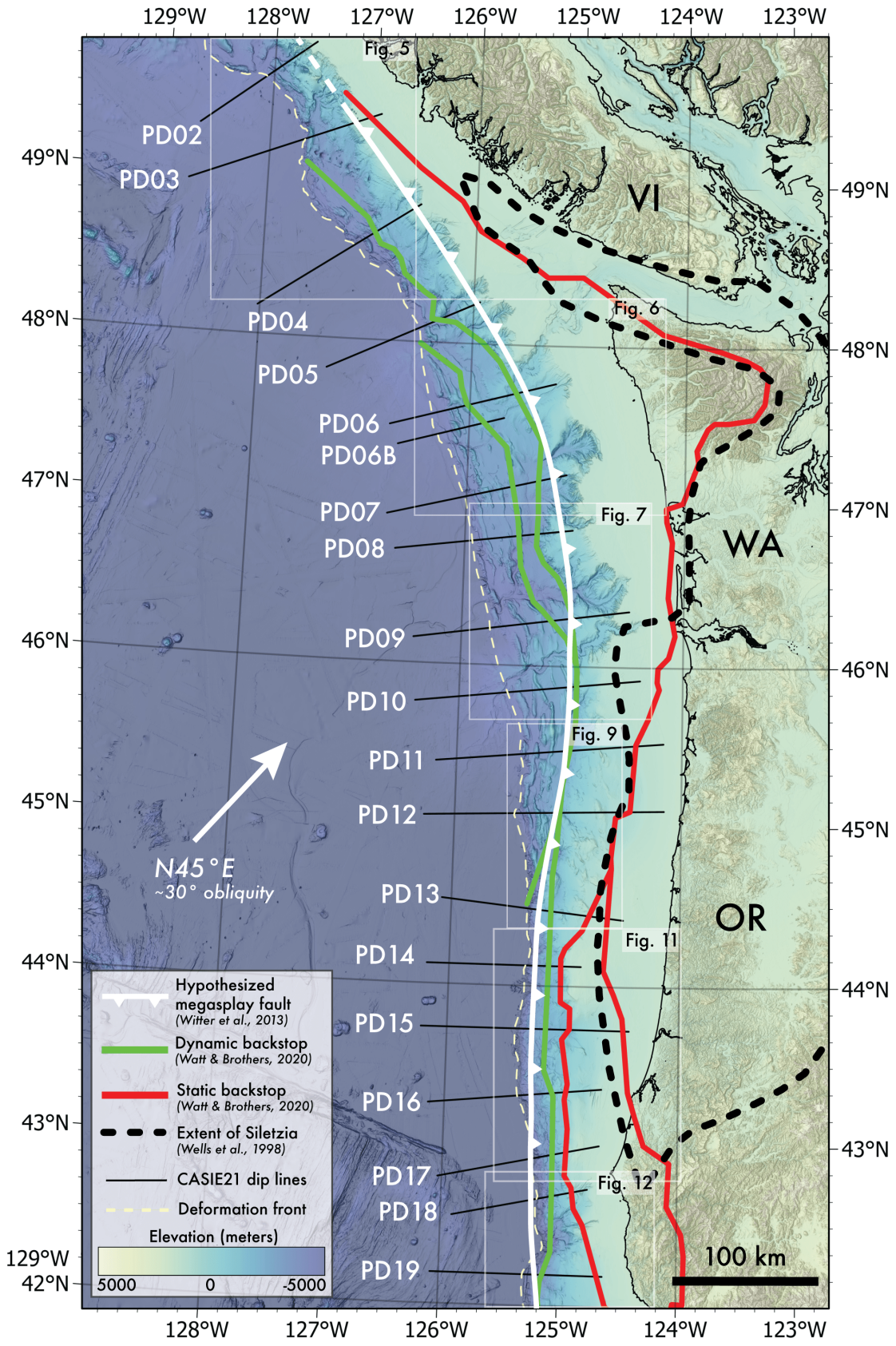

Figure 1 Elevation map of GMRT bathymetry compilation (Ryan et al., 2009) in meters for the region of the offshore Cascadia Subduction Zone overlain with the location of the hypothesized megasplay fault system from Witter et al. (2013), dynamic and static backstops (Watt and Brothers, 2020), Siletzia extent (Wells et al., 1998), CASIE21 dip lines (PD02 to PD19), and approximate deformation front location. Subduction vector and obliquity angle indicated on map (McCaffrey et al., 2007).

Geoscience Data System (MGDS) hosted by the Lamont-Doherty Earth Observatory of Columbia University (refer to Data and Code Availability Statement). Since the CASIE21 seismic data were acquired and processed with consistent workflows and parameters, this allows for direct comparison of seismic imaging features between lines. Analysis of CASIE21 seismic profiles is supplemented with 50m gridded bathymetry from the Global Multi-Resolution Topographic (GMRT) compilation (Ryan et al., 2009) and, where available, 30-m gridded U.S. Geological Survey (USGS) bathymetry (Dartnell et al., 2021, 2023) to evaluate the geomorphic expression of faulting related to the IOWTZ and connect the surface expression across 2D seismic profiles. Complementary and higher resolution sparker multi-channel seismic reflection data collected with the R/V Rachel Carson in 2019 (Balster-Gee et al., 2023) by the USGS is interpreted to evaluate near surface (i.e., upper ~1 km of the subsurface) evidence of fault activity within the IOWTZ and inner wedge domains. Joint interpretation of seismic reflection data at multiple scales of resolution allows us to more effectively connect deeper fault structure imaged by CASIE21 to near surface fault activity imaged within the USGS sparker seismic data. A complementary study by Ledeczi et al. (2024) provides a thorough evaluation of late Quaternary evidence for fault activity within the outer wedge domain using sparker seismic data. Through joint analysis of different geophysical datasets with multiple scales of resolution, this study refines the location and nature of the IOWTZ in the Cascadia accretionary wedge and evaluates evidence for an active, margin-spanning megasplay fault system in the vicinity of the IOWTZ in Cascadia.

2.3 Methods for mapping accretionary wedge domains

To locate the IOWTZ in the Cascadia accretionary wedge, we identify regional-scale changes in the overall structural style (2.3.1) and seismic character (2.3.2) of the wedge captured in CASIE21 dip profiles using *Kingdom Suite* software (refer to Data and Code Availability Statement).

2.3.1 Structural Style

Structural style is an observation of the dominant mode of subsurface deformation in a region due to a common tectonic origin (e.g., Harding and Lowell, 1979). Changes in the structural style of accretionary wedges provides insight into the history of wedge development and evolution (Breen et al., 1986; Flinch et al., 2003; Richter et al., 2007; Cook et al., 2014). Fault vergence, fault dip, thrust spacing, and faulting type from the CASIE21 data are used to characterize regional-scale trends in structural style in both the along-dip and along-strike direction. For example, in CASIE21 line PD04, the outer wedge domain is identified based on its structural style characterized by wide seaward verging, fault-propagation fold style thrust faulting (Fig. 2A). The inner wedge domain is identified based on its structural style characterized by closely spaced, imbricated thrust sheets dominated by seaward vergence (Fig. 2A). The IOWTZ is characterized as a zone between the inner and outer wedge with a gradational change in the observed structural style of the wedge with mixed vergence thrust faulting (Fig. 2A).

2.3.2 Seismic Character

Seismic character reflects the cumulative expression of subsurface physical and chemical properties and is inherently linked to both subsurface structural complexity and the presence and migration of subsurface fluids and gas (Moore et al., 1985; Jurado and Comas, 1992; Moore and Vrolijk, 1992; Lee et al., 1994; Berndt et al., 2004; Løseth et al., 2009). Changes in seismic character are identified primarily by changes in reflector coherency, which is a measure of the spatial continuity of seismic reflectors that depends on the level of scattering and attenuation of seismic energy in the subsurface (Li et al., 2021). We develop and employ a qualitative scale for seismic character ranging from "coherent" to "incoherent" (Fig. 2C). Decreasing seismic coherency has been inferred to represent increasing structural complexity of accretionary complexes (Cowan, 1985; Moore et al., 1985). For example, in CASIE21 line PD04, the seismic character of the incoming sediment is coherent, the seismic character of the outer wedge is mostly coherent to semi-coherent seismic character, the seismic character of the IOWTZ is semi-coherent to mostly incoherent, and the seismic character of the inner wedge is mostly incoherent to incoherent. This demonstrates a gradational decrease in seismic coherency across the IOWTZ (Fig. 2B). Additionally, throughout the entire accretionary wedge, there is a loss in seismic coherency with depth due to seismic attenuation and scattering (Fig. 2B). Together with our characterization of structural style, this example using CASIE21 line PD04 demonstrates how seismic character is linked with increasing structural complexity of the Cascadia accretionary wedge moving landward from the deformation front.

2.4 Methods for evaluating megasplay fault activity

Evidence for megasplay fault activity at the IOWTZ is evaluated for each of the identified along-strike segments and compared with the location and structure of the previously hypothesized megasplay fault. Evidence for megasplay fault activity is classified into three categories: positive, negative, or inconclusive. A classification of positive evidence indicates that a megasplay fault structure is observed at the IOWTZ and there is sufficient evidence to demonstrate recent fault activity. In this study, the same definition is used for "active" as that described in Ledeczi et al. (2024), where faults that either deform or offset inferred late Quaternary sedimentary horizons are classified as active. A classification of negative evidence indicates that a megasplay fault structure is observed at the IOWTZ in CASIE21 seismic profiles, but near surface observations from USGS sparker seismic profiles and available bathymetry provide conclusive evidence of no recent fault activity. A classification of inconclusive indicates that a megasplay fault

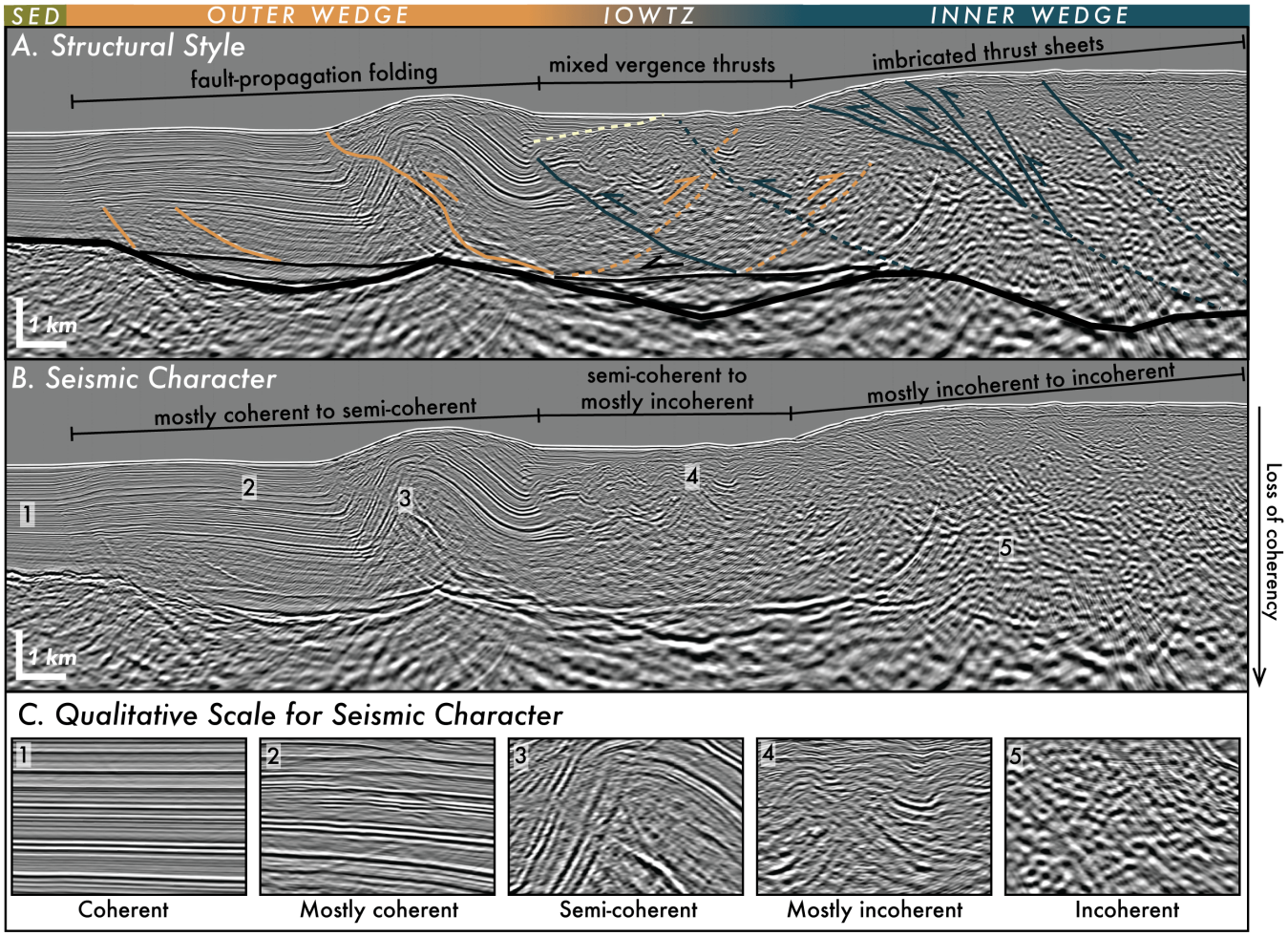

Figure 2 Structural style and seismic character methods. **A-B.** Example figures demonstrating methods for evaluating changes in **(A)** structural style and **(B)** seismic character of the Cascadia accretionary wedge using pre-stack depth migrated CASIE21 seismic profile PD04 (no vertical exaggeration) to delineate outer and inner wedge domains and the inner-outer wedge transition zone (IOWTZ). Also note seismic coherency decreases with depth in addition to in the along dip direction. **(C)** Seismic sections (~3x zoom) from PD04 profile demonstrating qualitative scale used for evaluating seismic character based on reflector coherency.

structure is observed in the given location; however, there is either a lack of near surface observations in that location or fault activity is ambiguous based on all existing data. In some locations along strike, a megasplay fault structure may not exist at the IOWTZ, neither active nor inactive.

3 Results

The spatial extent of the inner and outer wedge domains and the IOWTZ of the Cascadia accretionary wedge is mapped based on changes in structural style and seismic character observed in CASIE21 seismic profiles (Figs. 3, 4). The landward extent of the inner wedge domain (Fig. 3) is bounded by the seaward-most boundary of the combined Siletzia terrane from Wells et al. (1998) and the static backstop from Watt and Brothers (2020) (Fig. 1). We also document the approximate extent of wedge top sedimentary cover and incoming sediments (Fig. 4). Interpretations of plate boundary geometry and megathrust decollement used to guide our analysis of upper plate structures are consistent with or simplified from Carbotte et al. (2024). Based on changes in accretionary wedge structure and faulting, the wedge is classified into five along-strike segments: Northern Vancouver Island (~49.2-49.6°N; PD02), Central Vancouver Island (~48.3-49.2°N; PD03-04), Washington & Northern Oregon (~44.2-48.3°N; PD05-13), Central Oregon (~42.6-44.2°N; PD14-17), and Southern Oregon (~42-42.6°N; PD18-19) (Figs. 3, 4, Table 1). The Washington & Northern Oregon segment is further subdivided into three subsegments: Olympic (PD06-PD07), Astoria (PD08-PD09), Tillamook (PD10-PD12). In some locations, segment boundaries in accretionary wedge structure exhibit more spatially gradational changes in structure, and hence, are described as along-strike transition zones (ATZ) instead of distinct along-strike boundaries.

3.1 Northern Vancouver Island (~49.2-49.6°N)

The Northern Vancouver Island segment is situated at the northern terminus of the Cascadia subduction zone (Fig. 3). This segment of the accretionary wedge, which appears to be indented landward, has been previously interpreted as a structural transition (Watt and

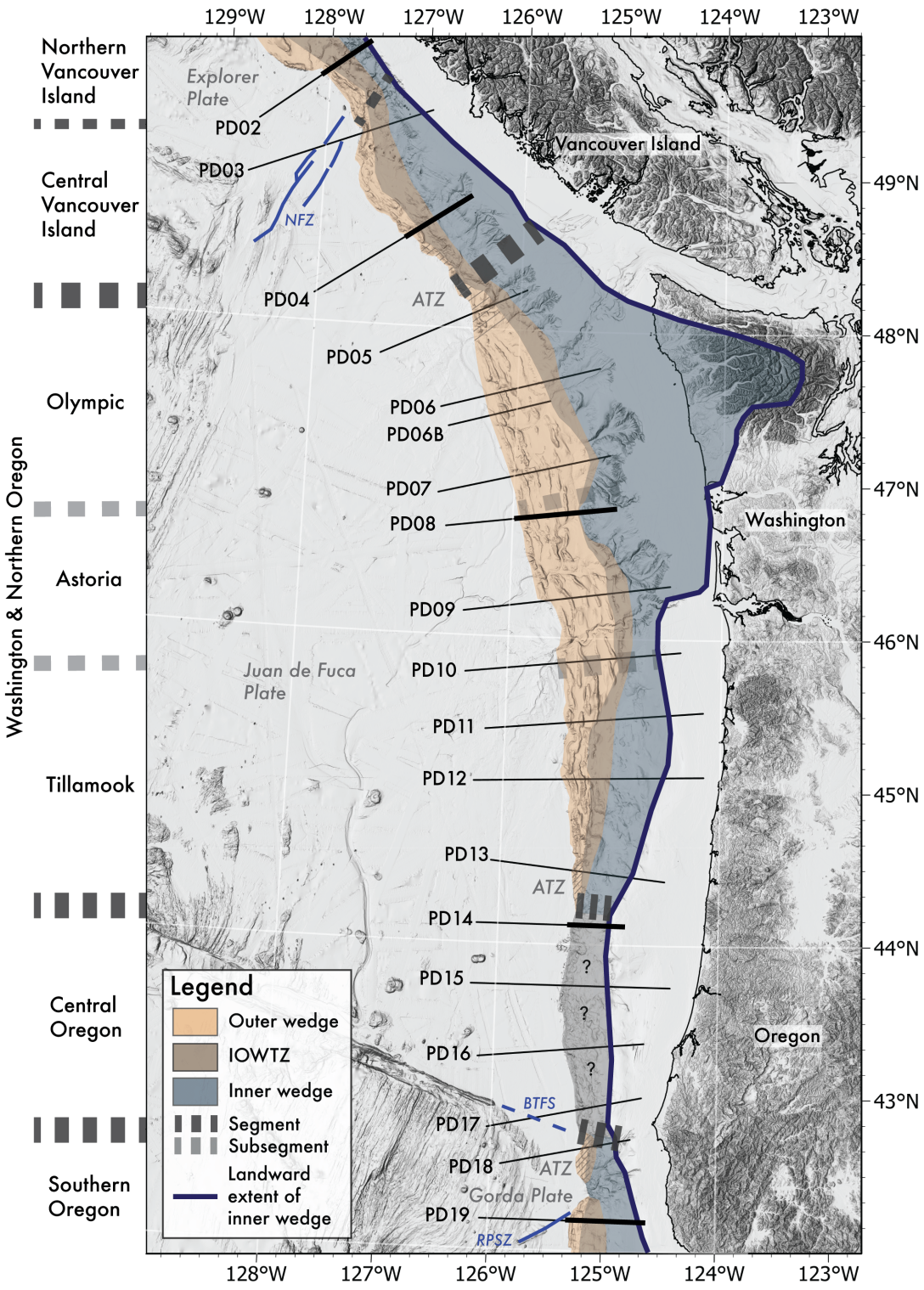

Figure 3 Hillshaded map of GMRT bathymetry compilation with results for spatial extent of outer wedge, inner wedge, and inner-outer wedge transition zone (IOWTZ). Grey hatching of the outer wedge domain indicates the extent of along-strike transition zones (ATZ). Along-strike segment and subsegment boundaries drawn with dark grey and light grey dashed lines, respectively (with line width corresponding to locational certainty of the boundary), landward extent of inner wedge drawn with thick blue line, CASIE21 dip lines drawn with fine black lines, and extent of seismic profiles presented in Figure 4 drawn with thicker black lines. Grey shading of the wedge with question marks indicates no outer wedge or IOWTZ domains can be identified. Blue lines show the location of relevant structures on the incoming plate. The grey domain with a question mark indicates no inner, outer, or IOWTZ domains can be identified. NFZ is Nootka Fault Zone, BTFS is Blanco Transform Fault System, RPSZ is Rogue Propagator Shear Zone.

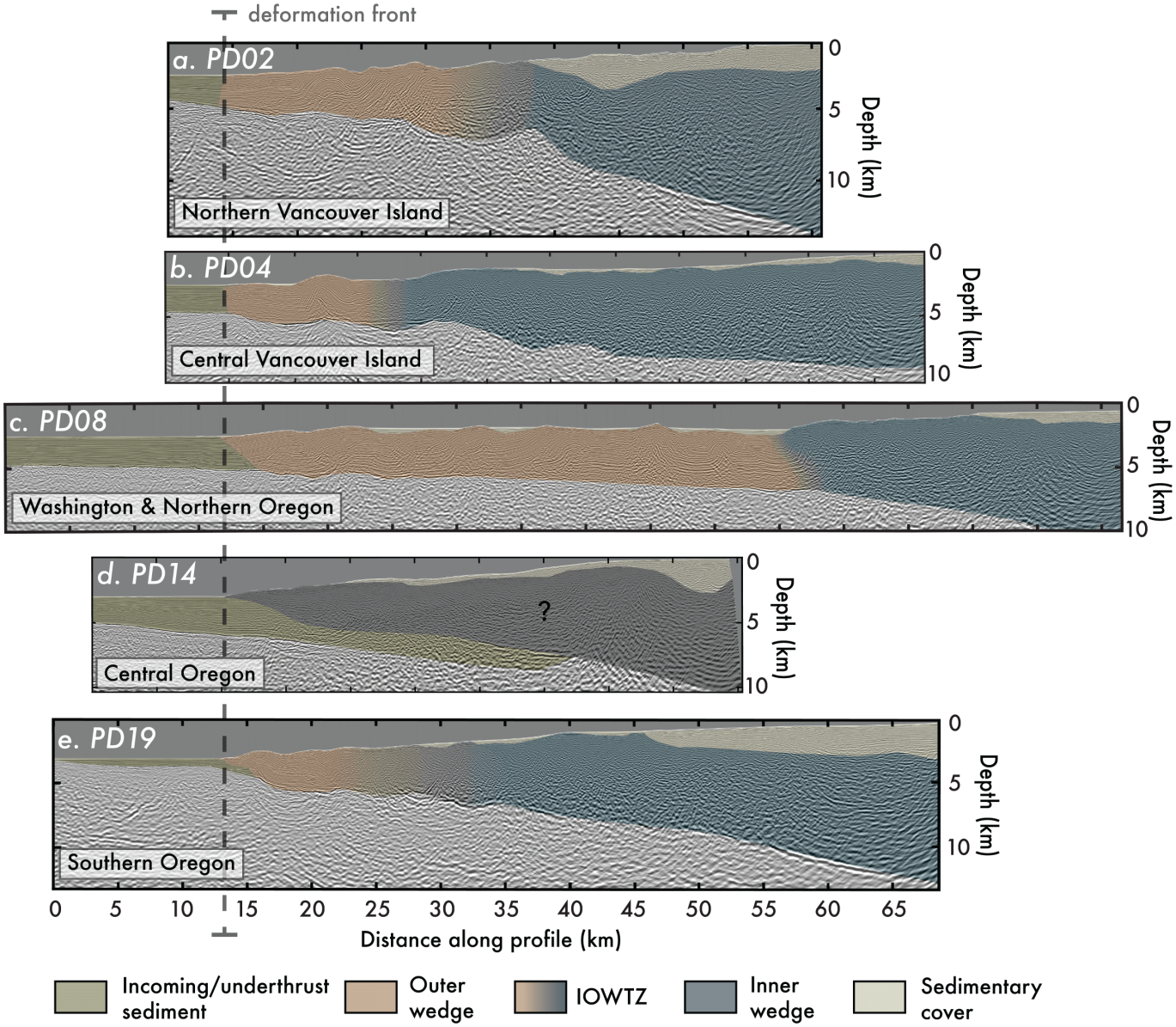

Figure 4 Representative examples of CASIE21 seismic profiles from each along-strike segment showing wedge structural domains. **a-e.** Overlain with semi-transparent masks delineating the interpreted incoming/underthrust sediment (green), outer wedge (orange), inner wedge (blue), IOWTZ (orange-blue gradient), sedimentary cover (yellow), and downgoing igneous basement crust of the Juan de Fuca plate (white). The grey domain with a question mark indicates no inner, outer, or IOWTZ domains can be identified. Extent of CASIE21 seismic profiles is indicated by thick black lines in Figure 3. Plate boundary and decollement interpretations simplified from Carbotte et al. (2024).

Brothers, 2020) corresponding to the location where the Nootka Fracture Zone (NFZ) intersects the margin (Rohr et al., 2018; Hutchinson et al., 2023) (Fig. 5a). CASIE21 line PD02 images the ~7 km wide IOWTZ in this segment and captures drastically different wedge structure compared to that of the Central Vancouver Island segment in lines PD03 and PD04 (Fig. 5b-g). This is expected given that PD02 captures the upper-plate structure atop the more steeply dipping Explorer Plate (Carbotte et al., 2024). The outer wedge in PD02 is dominated by imbricated, landward-verging fault-propagation fold style thrust sheets with mostly coherent reflectivity (Fig. 5b). The plate hinge identified by Carbotte et al. (2024), where the dip of the downgoing plate abruptly steepens, is located near the seaward end of the IOWTZ within the outer wedge domain (Fig. 5b). The inner wedge in PD02 exhibits incoherent reflectivity and has an overlying sedimentary sequence that thickens landward from the IOWTZ. Characterizing structure within the IOWTZ zone is difficult due to mostly incoherent reflectivity; however, there is evidence for landward-dipping reflectors with a linear pattern (i.e., seismic lineations) that may represent potential seaward-verging megasplay faults at the IOWTZ. It is unclear whether these seismic lineations reach the near surface due to poor coverage in our available bathymetry and the highly channelized seafloor in this location. Local basement topography was observed in the downgoing Juan de Fuca plate by Shuck et al. (2023) and Carbotte et al. (2024) at the IOWTZ and was interpreted as a tear in the downgoing slab (Fig. 5b). The observed landward-dipping seismic lineations of the IOWTZ appear to sole

near the top of this topographic structure (Fig. 5b). Based on a lack of coherent reflectivity at the IOWTZ in PD02, we cannot confidently determine whether an active out-of-sequence megasplay fault system exists in this location.

3.2 Central Vancouver Island (~48.3-49.2°N)

Both CASIE21 lines PD03 and PD04 exhibit similar overall wedge structural style and seismic character (Fig. 5e, g). In both lines, the outer wedge consists of a single major seaward-verging fault-bend fold style thrust sheet that accretes all or nearly all of the incoming sediment section to the wedge. The seismic character of the outer wedge is mostly-coherent with well-imaged, continuous reflectors offset by the frontal thrust fault. The inner wedge captured by PD03 and PD04 exhibits mostly-incoherent to incoherent reflectivity with closely spaced, dominantly seaward-verging thrust fault structures and landward dipping seismic lineations. The IOWTZ is characterized by a zone of doubly-verging thrust faults. Seaward-verging thrust faults of the inner wedge domain deform landward-verging thrust faults of the outer wedge domain. Landward of this change in fault vergence adjacent to the IOWTZ, inner wedge faults in both seismic profiles have a clear expression at the seafloor observable in both the seismic and bathymetric data (Fig. 5c,d,f). PD03 has a wider IOWTZ where individual inner wedge faults appear to disturb and tilt overlying sediments and deform the seafloor between 10 and 30 km distance along the seismic section (Fig. 5c-e; white triangles). In some locations, these faults also exhibit distinct fault plane reflections with reverse polarity (Fig. 5d). PD04 has a narrower zone of faulting between 20 and 30 km distance along the seismic section where deformation is more focused (Fig. 5f-g; white triangles). In PD04, faults at the IOWTZ are locally associated with both a steeper wedge slope and lack of overlying sediment cover (Fig. 5f). These faults are classified as megasplay faults because inner wedge faults appear to deform younger outer wedge material, providing evidence for out-of-sequence fault activation in this zone, and because these faults coincide with the boundary between the coherent and incoherent seismic character of the wedge. Additionally, these faults show evidence of surface expression at the seafloor in the GMRT 50-m bathymetry (Fig. 5a) while connecting with the megathrust fault at depth (Fig. 5e,g). The coherence of seismic reflectors decreases with depth, particularly in line PD04 between 25-30 km along the seismic section, making it difficult to identify the exact points in the subsurface at which faults sole into the megathrust fault (Fig. 5g). The trace of these megasplay faults in the bathymetry is discontinuous; however, the faults all generally trend in the same direction and extend over ~50 km along strike (Fig. 5a). This system of megasplay faults at the IOWTZ is located on average ~10-30 km southwest of the previously proposed megasplay fault trace of Witter et al. (2013) (Fig. 5a). The plate hinge identified by Carbotte et al. (2024) coincides with this megasplay fault system in PD04 (Fig. 5g; green star). However, in PD03, the plate hinge is not associated with the identified megasplay fault system and is instead located further east beneath a major slope break coincident with the location of the previously hypothesized megasplay fault by Witter et al. (2013) (Fig. 5e; green star). Further acquisition and analysis of higher resolution seismic and bathymetric data is needed in this segment to determine the recency of megasplay fault activity; therefore, the evidence for activity of this megasplay fault system captured in PD03 and PD04 is classified as inconclusive.

3.3 Washington & Northern Oregon (~44.2-48.3°N)

The Washington & Northern Oregon segment, imaged by CASIE21 profiles PD05-PD13, is defined by the extent of the landward vergence zone and is the longest of the identified segments, spanning ~400 km along strike (Fig. 3, Table 1). This segment exhibits a widening and then narrowing of the outer wedge domain at the northern and southern ends of this segment, with the widest point near line PD07 spanning ~65 km between the deformation front and the beginning of the IOWTZ (Fig. 3). The structural style of the outer wedge domain in this segment is characterized by landward-dominated mixed vergence thrust faulting (Fig. 4c). This segment exhibits the most internal variation in accretionary wedge structure of all the identified segments, especially at the IOWTZ. Based on this, this segment is further subdivided into three subsegments (Olympic, Astoria, Tillamook; Fig. 3). PD05 and PD13 capture ATZs where wedge structure and faulting exhibits gradational changes across segment boundaries, and hence, these profiles contain structural features in common with adjacent segments and subsegments.

3.3.1 Olympic Subsegment (PD05, PD06, PD07)

PD05 is located within an ATZ where key structural features are present from both adjacent segments (Fig. 3, Table 1), including landward-verging outer wedge thrust faults, typical of the Washington & Northern Oregon segment, and a megasplay fault system reaching near the surface, typical of the Central Vancouver Island segment. The IOWTZ in line PD05 is characterized by a zone of mixed vergence where landward-verging thrust faults of the outer wedge domain overlap with seaward-verging faults of the inner wedge domain (Fig. 6c). A decrease in the coherency of seismic character from semi-coherent to mostly incoherent occurs across the IOWTZ. Adjacent to the IOWTZ, a series of seaward-verging inner wedge thrust faults dipping at ~33° sole near the megathrust fault at depth (Fig. 6c). At the surface, these faults coincide with a slope break in the bathymetry and tilted wedge top sediments (Fig. 6b). At depth, the faults correspond with a steepening of the downgoing plate dip (i.e., plate hinge), and an along-dip shallowing of the plate boundary decollement (Carbotte et al., 2024) (Fig. 6c). Therefore, these inner wedge faults are interpreted as a system of megasplay faults associated with the IOWTZ. The near surface expression of this megasplay fault system is disrupted by a

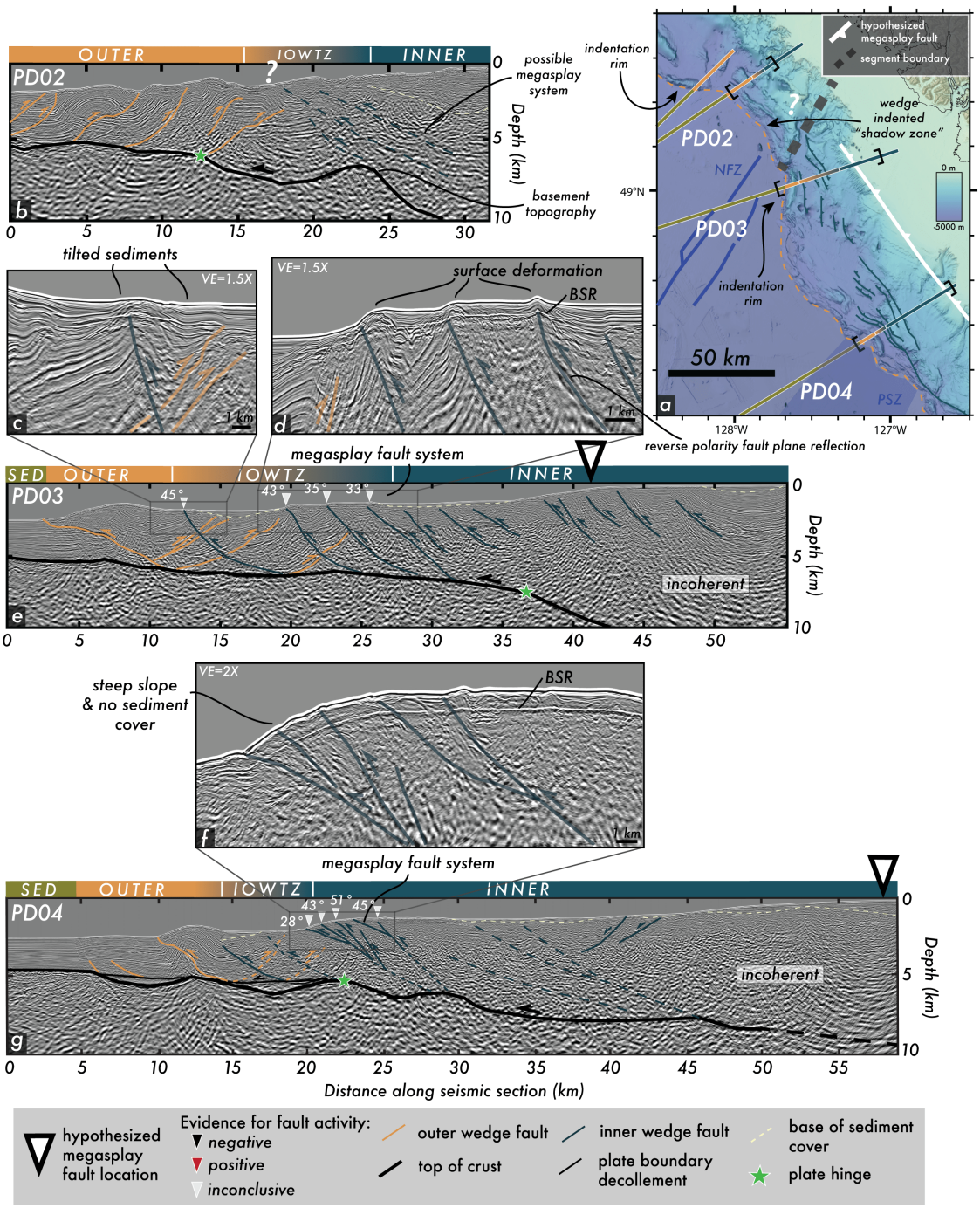

Figure 5 The Northern and Central Vancouver Island segments. **a.** Map of GMRT bathymetry with locations of corresponding CASIE21 seismic images, segment boundaries, and megasplay fault location hypothesized by Witter et al. (2013). Seismic image extent is indicated on the map by black brackets. Fine blue lines in the map correspond with megasplay faults of the inner wedge domain as interpreted in seismic images. Thick blue lines show the location of the Nootka Fault Zone (Rohr et al., 2018). **b-g.** Orange color represents the outer wedge, blue color represents inner wedge, orange-blue gradient represents inner-outer wedge transition zone (IOWTZ), and green color represents incoming sediment section. Dotted lines represent less certain fault interpretations. Simplified top of crust, plate boundary decollement, and plate hinge interpretation is from Carbotte et al. (2024). Previously hypothesized splay fault location is from Witter et al. (2013). Smaller triangles in the seismic sections indicate the position of interpreted megasplay faults at the IOWTZ and are color-coded by evidence for fault activity. No vertical exaggeration of seismic images. Bottom-simulating reflector (BSR) is indicated on seismic images.

deep seafloor channel that cuts across the accretionary wedge in this location (Fig. 6a); therefore, evidence for activity of these megasplay faults at the IOWTZ in PD05 is classified as inconclusive. Nevertheless, these faults should be considered as candidate active megasplay faults at the IOWTZ and a potential focus for more detailed near-surface investigations to evaluate deformation of wedge top sediments. PD05 does not inter-

sect the trace of the Witter et al. (2013) megasplay fault; however, the IOWTZ has been identified within the extent of the seismic profile and there is no clear surface expression of faulting in the GMRT bathymetry at the location of the Witter et al. (2013) splay fault trace that would suggest a megasplay fault exists at that location (Fig. 6a).

In line PD06, the IOWTZ is buried by a 1-2 km thick layer of undeformed sediment (Fig. 6d). No faults are mapped at the IOWTZ in this location by a recent sparker investigation of near surface splay fault activity (Ledeczi et al., 2024). However, at depth, 2-3 seaward-verging inner wedge thrust faults dipping at 30° and 42° are observed to offset folded strata of outer wedge thrust sheets at the IOWTZ between 7 to 20 km distance along the seismic section (Fig. 6d-e). The IOWTZ also corresponds with a local shallowing of the plate boundary decollement (Carbotte et al., 2024) inferred to cut across the base of these inner wedge thrust faults (Fig 6e). These faults are interpreted as megasplay faults due to their apparent out-of-sequence reactivation because they appear to have deformed more recently accreted outer wedge material but are now no longer active as evidenced by undeformed overlying sediment (Fig. 6d). Within the inner wedge at ~25 km along the seismic section, there is a pair of conjugate faults that are also buried by ~1 km of undeformed sediment (Fig. 6e). This thick layer of undeformed sediment cover atop the wedge indicates a lack of recent activity on megasplay faults and other inner wedge splays in the location of PD06. Without information on sedimentation rate, we cannot estimate when these faults were last active; however, it is likely on the order of tens (if not hundreds) of thousands of years. This result is inconsistent with the hypothesis for active megasplay fault in this location.

Three isolated fault structures between PD06 and PD07 captured only in the bathymetry at the location of the mapped IOWTZ are expressed at the seafloor just south of the Quillayute submarine channel (Fig. 6a). The westernmost fault of the three faults has been classified as Quaternary active by Ledeczi et al. (2024). These faults are short in length, isolated to a small area, do not plausibly connect to surrounding structures captured in adjacent CASIE21 seismic profiles, and do not appear to offset adjacent submarine channels. Further MCS surveying is needed in this location to determine the deeper structure of these faults and whether they are connected to the megathrust fault at depth.

In line PD07, a single seaward-verging thrust fault steeply dipping at 47° within the IOWTZ represents a candidate megasplay fault (Fig. 6g). This fault is located ~5 km west of the megasplay fault trace from Witter et al. (2013). The location of this fault at the IOWTZ corresponds with a steepening of the downgoing plate dip (Carbotte et al., 2024) and an increase in wedge surface slope (i.e., wedge taper angle) (Fig. 6g). This fault offsets folded strata within the hanging wall of a landward-verging thrust sheet of the outer wedge domain (Fig. 6f). However, the fault is partially buried by a ~1-km thick layer of sediment at the seafloor (Fig. 6f), indicating a lack of recent activity. This result is consistent with Ledeczi et al. (2024) who also found no evidence for late Quaternary activity on this fault in their analysis of sparker seismic data. Therefore, evidence for recent activity on this megasplay fault structure at the IOWTZ is concluded as negative.

There is no evidence to suggest there is a continuous, active megasplay fault system in the Olympic subsegment imaged by CASIE21 lines PD05-PD07 as previously suggested by Witter et al. (2013). In PD05, subsurface structures indicate a megasplay fault system is likely present at the IOWTZ; however, evidence for recent activity of this fault system is inconclusive. Megasplay faults identified within lines PD06 and PD07 of the Olympic subsegment are buried by up to 2 kilometers of undeformed sediment, exhibit a discontinuous surface expression, and cannot be plausibly connected to the megasplay fault system identified in PD05. Overall, fault structure at the IOWTZ varies substantially from PD05 to PD07 and no active megasplay faults can be connected along-strike through this region based on similarities in fault surface expression and subsurface fault structure at the IOWTZ (Fig. 6).

3.3.2 Astoria Subsegment (PD08, PD09, PD10)

PD08 captures the best evidence for an active megasplay fault system at the IOWTZ within the Washington & Northern Oregon segment. The IOWTZ captured in PD08 is less of a zone, and instead a sharp boundary between the inner and outer wedge domains (Fig. 7a-b). A seaward-verging thrust fault system dipping at ~28° is present at this inner-outer wedge boundary and merges with the megathrust fault at depth while also extending up to the seafloor (Fig. 7b). At the seafloor, this fault system is expressed as two distinct fault scarps in the USGS 30-m bathymetry (Fig. 8c). At depth, this megasplay fault structure exhibits a highly deformed zone with mostly incoherent reflectivity, representing a well-developed fault system with numerous branching fault strands (Fig. 8b). The surface trace of these faults extends ~50 km along strike and is co-located with large seafloor slope failures identified by Hill et al. (2022). This megasplay fault system is located ~20 km west of the previously hypothesized splay fault system (Fig. 7a). This fault system does not appear to connect with structures further north in PD07, primarily because of a lack of evidence in the bathymetry due to the extensive seafloor erosion by the Grays submarine channel between PD07 and PD08 (Fig. 7a). This fault is also coincident with an unusual, convex-outward boundary between the inner and outer wedge domains (Fig. 8a) as well as with a relatively undeformed zone with extremely flat wedge taper seaward of the fault system within the outer wedge domain (Fig. 7b, 8b). Submarine channels Grays and Guide appear to be routed to the north and south around this major morphologic feature (Fig. 8a). Near surface evidence for late Quaternary activity on this fault system from nearby sparker data remains inconclusive because the steep slope associated with this structure that acts as a sediment bypass, preventing sedimentation of the slope (Ledeczi et al., 2024). Therefore, activity on this megasplay fault system is likely, but activity is currently inconclusive based

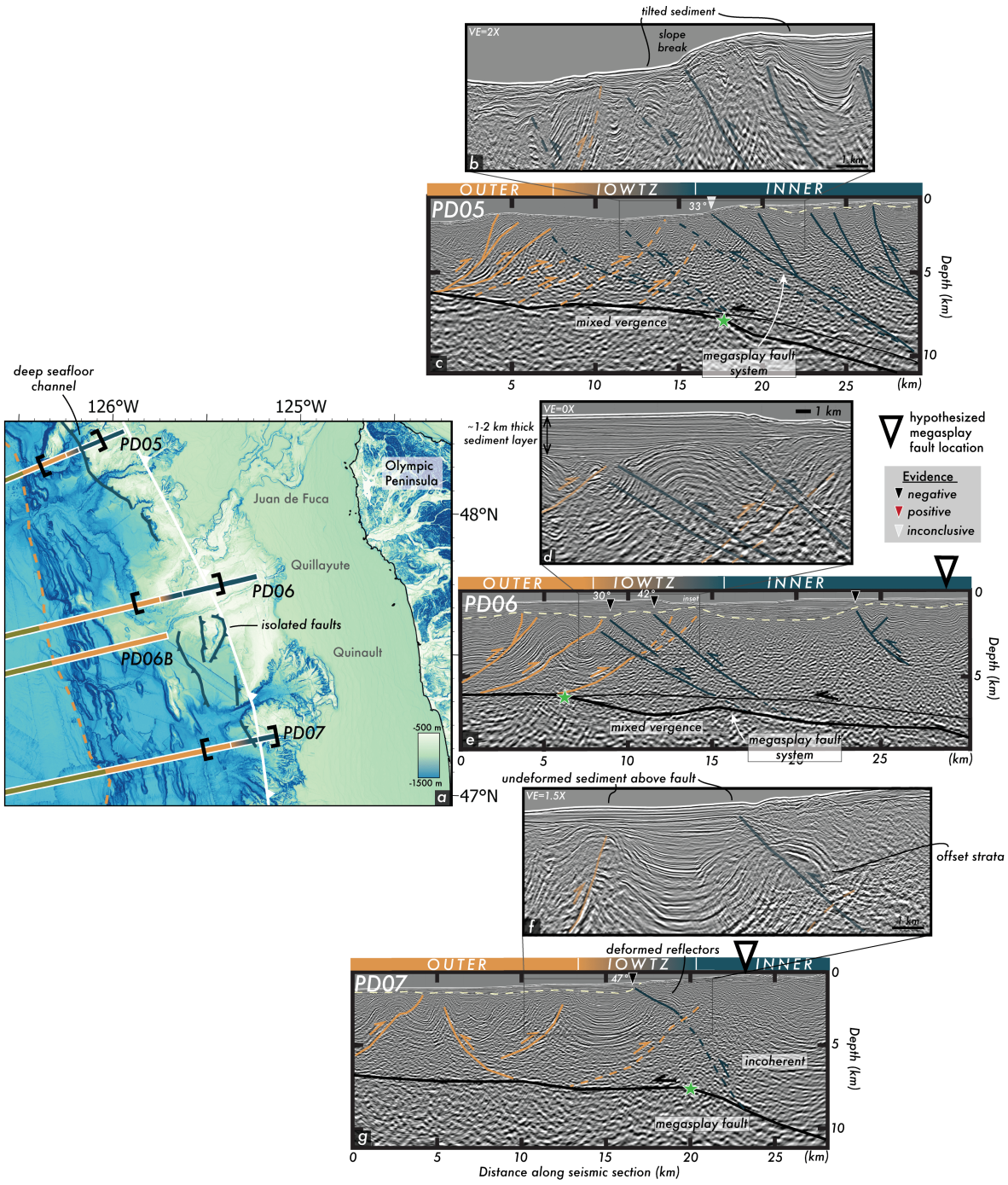

Figure 6 Olympic subsegment of Washington and Northern Oregon segment. Symbology is the same as Fig. 5. **a.** Map of 30-m USGS bathymetry. **b-g.** Seismic panels from CASIE21 seismic lines PD05, PD06, and PD07 showing deep and shallow fault structure.

on available evidence.

PD09 crosses a similar slope break and increase in the seafloor elevation that can be traced south in the bathymetry across the Guide and Willapa submarine channels from the potentially active megasplay fault system identified in PD08 (Fig. 7a, e). This break in the seafloor corresponds with a seaward-verging thrust fault within the IOWTZ that has a similar structural style to faults within the outer wedge domain. This fault is dipping at 35° and soles into the megathrust fault at depth (Fig. 7e). This structure is classified as a megasplay fault due to its apparent out-of-sequence activity and apparent connectivity with the megasplay fault system identified in PD08. However, unlike the megasplay fault system identified in PD08, there is conclusive evidence from sparker seismic data that this megasplay fault in PD09 is not recently active based on a lack of deformation in overlying sediments (Ledeczi et al., 2024). Two additional thrust faults within the IOWTZ are identified; however, these faults exhibit no expression at the seafloor and are also blanketed by a layer of undeformed sediments (Fig. 7c, e; black triangles).

PD10 is located at the Astoria-Tillamook subsegment boundary defined by where a megasplay fault structure is no longer observed, neither active nor inactive. Instead, a system of active right-lateral strike-slip faults

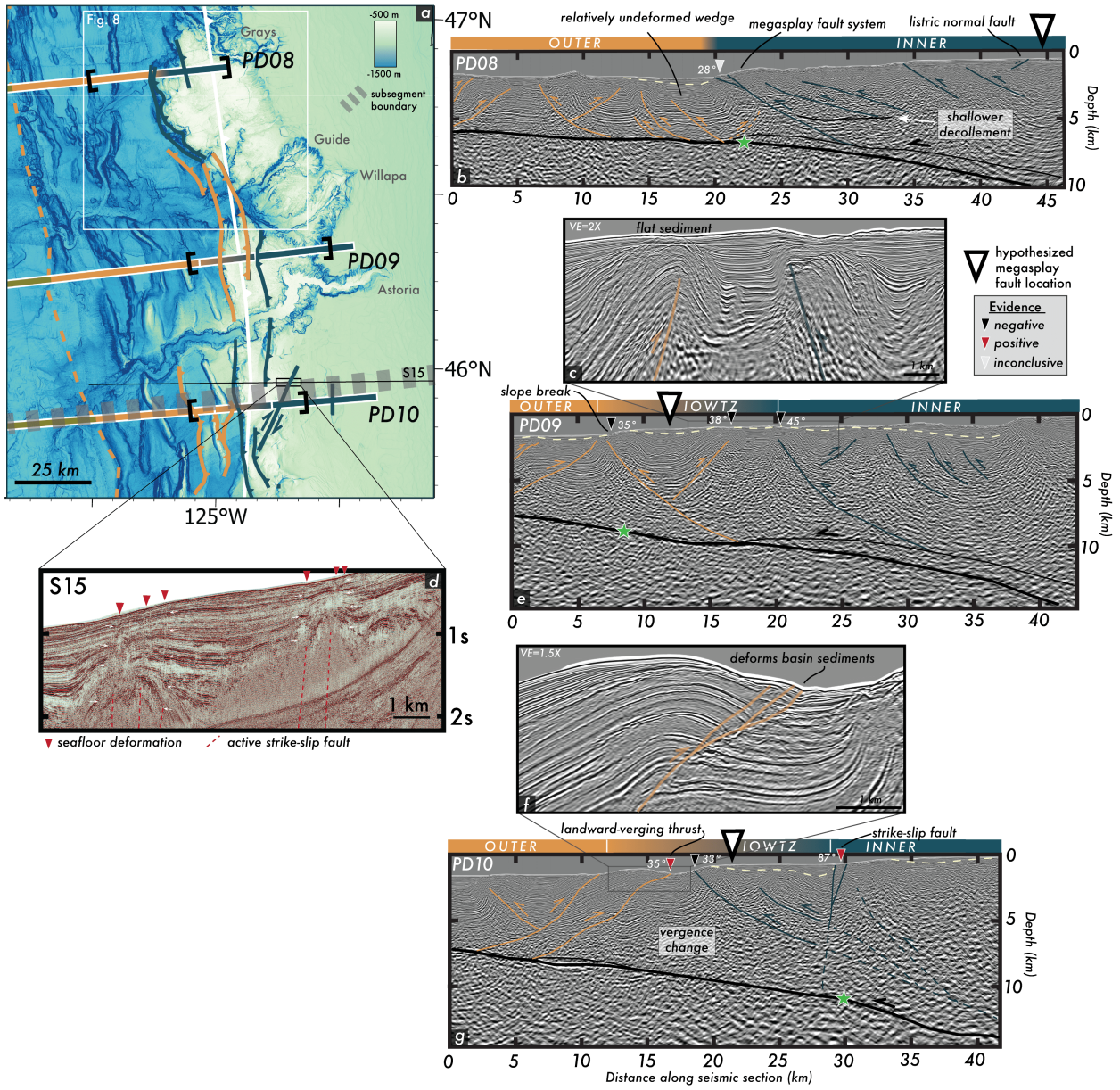

Figure 7 Astoria subsegment of Washington & Northern Oregon segment, including the Astoria-Tillamook subsegment boundary. Symbology is the same as Fig. 5. **a.** Map of 30-m USGS bathymetry. Continental shelf shown in light green color. White inset box shows the region of Fig. 8. Subsegment boundary shown by grey dashed line. **b-g.** Seismic panels of CASIE21 seismic lines PD08, PD09, and PD10 and USGS sparker seismic line S15 showing accretionary wedge structure and near surface fault deformation.

and a landward verging thrust fault are observed at the IOWTZ (Fig. 7g). Thrust fault vergence at the IOWTZ in PD10 changes from dominantly landward within the outer wedge domain to seaward within the inner wedge domain. A landward-verging thrust fault in the IOWTZ dipping at 35° is observed to reach the surface and deform wedge top basin sediments while also connecting with the megathrust at depth (Fig. 7f-g). Consistent with these observations, Ledeczi et al. (2024) found this fault to exhibit evidence for late Quaternary activity in sparker data. Landward of this fault, a seaward-verging inner wedge thrust fault dipping at 33° is observed at the IOWTZ near the megasplay fault trace hypothesized by Witter et al. (2013). This fault is associated with a slope break in the seafloor (Fig. 7g; black triangle) and appears to reach the surface; however, it is found to be conclusively not active based on near surface observations of basin sediments (Ledeczi et al., 2024). Additionally, it is unclear where this fault soles in the subsurface due to a lack of coherent reflectivity at depth (Fig. 7g). At the boundary between the IOWTZ and the inner wedge domain, an active right-lateral strike slip fault system is present and extends ~25 km along strike. This strike-slip fault is dipping at 87° and crosscuts two adjacent inactive seaward-verging thrust faults (Fig. 7g; red triangle). This fault is associated with a more gradual increase in seafloor elevation and is roughly co-located with the plate hinge from Carbotte et al. (2024) (Fig. 7g; green star). At the seafloor, this fault exhibits evidence for deformation of near surface sediments captured in sparker seismic line S15 just to the north of line PD10 (Fig. 7a, d). This provides positive evidence for late Qua-

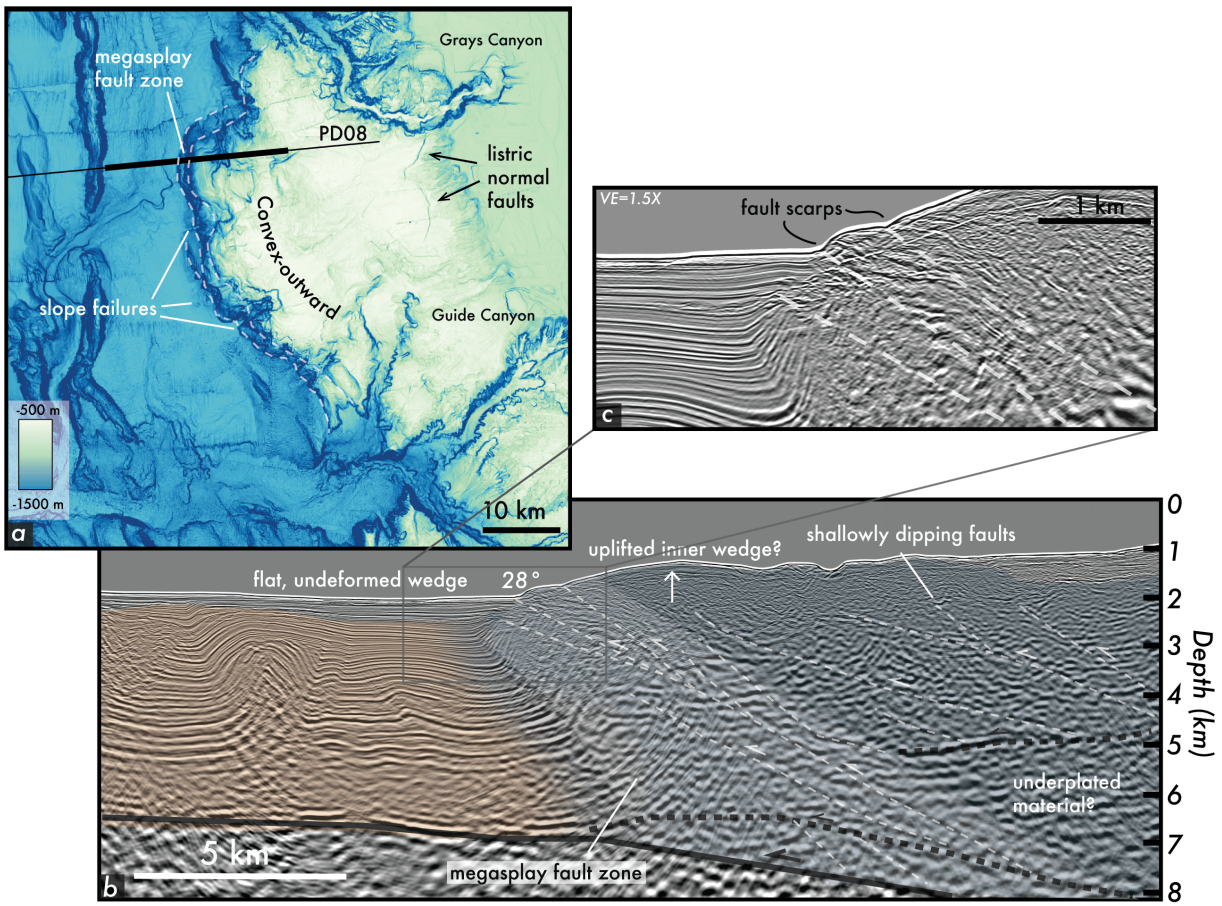

Figure 8 IOWTZ megasplay fault system captured by CASIE21 line PD08 of Astoria subsegment. **a.** Detailed map of USGS 30-m bathymetry. Continental shelf shown in light green color. Thicker black on PD08 line shows the extent of the seismic image shown in this figure. White dashed lines on the map indicate the surface trace of the megasplay fault interpreted at depth. White shaded area between the outer (orange) and inner (blue) wedge domains indicates our proposed megasplay fault zone. No vertical exaggeration on seismic image.

ternary activity on this strike-slip fault at the IOWTZ. Both active faults identified within the IOWTZ captured by PD10 do not exhibit typical megasplay fault structure, suggesting that a more complex style of wedge deformation is occurring at the IOWTZ in this location and an overall change in faulting style at the Astoria-Tillamook subsegment boundary.

Within the Astoria subsegment captured by CASIE21 lines PD08 and PD09, a seaward-verging megasplay fault system is associated with the IOWTZ. This fault system is prominently expressed at the seafloor and continuous along strike (Figs. 7a, 13). However, this fault system is observed to have either negative or inconclusive evidence for recent activity. In PD10, at the Astoria-Tillamook subsegment boundary, CASIE21 and sparker seismic data provide evidence that both a landward-verging thrust fault and a strike-slip fault system are active at the IOWTZ. Overall, faulting at the IOWTZ in this region varies greatly over relatively short along strike distances (on the order of tens of kilometers) and evolves from dominantly thrust faulting to strike-slip faulting at the Astoria-Tillamook subsegment boundary. Megasplay faults in this region may be locally active at the structure identified in PD08; however, more high-resolution geophysical observations are needed to confirm recency of activity on this fault.

3.3.3 Tillamook Subsegment (PD11, PD12, PD13)

At the beginning of the IOWTZ captured by PD11, a landward-verging thrust fault, dipping at 34°, shows evidence for late Quaternary activity (Fig. 9a, c; red triangle) (Ledeczi et al., 2024). Landward of this fault, an active strike-slip fault system is present within the IOWTZ between 30 to 35 km distance along the profile (Fig. 9a, c; red triangle). CASIE21 line PD11 and sparker line S19 are roughly co-located, allowing for comparison of this strike-slip fault system in both seismic profiles of differing resolutions (Fig. 9a). In sparker line S19, seafloor sediments are deformed by two high-angle subsurface faults with opposing dips (Fig. 9b). This surficial deformation corresponds to a positive (transpressional) flower structure that is linked to this strike-slip fault system in PD11 (Fig. 9c). Landward of this flower structure, there is a near-vertical truncation of deep basin sediments associated with the IOWTZ at depth and an almost complete loss of coherence landward of this strike-slip fault system (Fig. 9c). Within the inner wedge, there is faint evidence for seaward-verging thrust faults that corresponds to mostly buried ridges at the surface; however, the lack of seismic coherence prevents detailed in-

terpretation of these structures (Fig. 9c).

Between CASIE21 lines PD11 and PD12 and within the inner wedge domain near the IOWTZ, another strike-slip fault system is present (Fig. 9a). This fault trends in the same direction as the two active strike-slip faults imaged in PD10, PD11 and S19. A distinct, and apparently young, seafloor scarp in the USGS 30-m bathymetry at this location offsets older seafloor ridges in a right-lateral sense of motion (Fig. 10b). Based on this observation, this fault system and the adjacent strike-slip faults captured in PD10 and PD11 likely comprise a larger-scale system of active right-lateral strike-slip faults in this region. Sparker line S58 captures the main strand of this active strike-slip fault. In the subsurface, a near-vertical strike-slip fault deforms the seafloor where the primary fault scarp is observed in the bathymetry (Fig. 10a-b; large red arrow). This fault is associated with multiple subsidiary normal faults that offset basin sediments adjacent to this structure (Fig. 10a, small red arrows). One of these normal faults exhibits significant offset of a buried and inactive ridge. The presence of normal faults surrounding the main fault strand indicate a negative (transtensional) flower structure in this location, as opposed to the positive flower structure observed in PD11 (Fig. 9c).

In PD12, thrust faults sole into a shallower decollement above the top of crust (Fig. 9e) (Carbotte et al., 2024). A change in thrust fault vergence from landward to seaward defines the beginning of the IOWTZ. There is no evidence for a seaward-verging megasplay fault structure at the IOWTZ in PD12, and instead there is an out-of-sequence landward-verging fault, dipping at 32°, that is overthrust onto a seaward-verging thrust fault at the IOWTZ (Fig. 9e). This fault cuts across folded strata of this seaward-verging thrust and appears to disturb sediments near the seafloor (Fig. 9d). There is a data gap in PD12, so interpretation of deeper fault structure in this location is based on information from surrounding seismic lines. It is inconclusive whether this overthrust landward-verging fault remains active at present (Fig. 9e; white triangle). Within the IOWTZ between 22 km to 35 km, four thrust sheets exhibit similar structure and vergence (Fig. 9e). However, the reflectivity of the strata comprising the two seaward-most outer wedge thrust sheets is more coherent than the reflectivity of the two landward-most inner wedge thrust sheets. This transition in subsurface seismic character defines the extent of the IOWTZ. A similar pattern occurs in PD13, where thrust sheets exhibit similar structural vergence, but different seismic character expressed as decreasing reflectivity moving landward across the profile (Fig. 9g). This enables the delineation of an outer wedge domain in PD13 without a major transition in structural style. In PD13, there is also an abrupt termination of the underthrust sediment section at ~30 km along the seismic section (Fig. 9g) attributed to a possible subducted seamount atop the downgoing Juan de Fuca plate (Carbotte et al., 2024). This pattern in PD12 and PD13, along with the presence of subducted seamounts near the southern end of the Washington & Northern Oregon segment, reflects the narrowing of the outer wedge domain and IOWTZ at the boundary of the Central Oregon segment and corresponds to the interpreted ATZ (Fig. 3). In PD13, two breaks in the seafloor within the IOWTZ are associated with two seaward-verging inner wedge thrust faults at depth (Fig. 9f-g; white triangles). These faults are potential megasplay fault structures; however, it is inconclusive whether these faults are active.

From CASIE21 line PD11 to PD13, the IOWTZ is roughly co-located with the proposed Witter et al. (2013) megasplay fault trace (Fig. 9a). However, fault structure, including fault type, fault vergence, and fault activity, within the IOWTZ is highly variable across these three seismic profiles. South of PD10 and within the Tillamook subsegment, there is a system of active right-lateral strike-slip faults at the IOWTZ along with an active landward-verging splay fault, but no seaward-verging megasplay fault structure is present. PD13 captures an ATZ where structure of the accretionary wedge features both an identifiable outer wedge domain characteristic of the Washington & Northern Oregon segment, but also an underthrust sediment section characteristic of the Central Oregon segment. This result reflects similar overarching conclusions from our analysis of the Washington & Northern Oregon segment that splay fault structure at the IOWTZ cannot be described by a single, active seaward-verging thrust fault that spans continuously along strike, as previously hypothesized.

3.4 Central Oregon (~42.6-44.2°N)

The Central Oregon segment is captured by CASIE21 lines PD14-PD17 (Fig. 11a). ATZs are captured by PD13 and PD18 at either end of this segment where there are key structural features in common with adjacent wedge segments to the north and south (Fig. 3). The Central Oregon segment is uniquely characterized by a lack of an identifiable outer wedge domain based on changes in structural style and seismic character of the wedge (Fig. 11b, Table 1). Instead, the entire accretionary wedge in this segment resembles the inner wedge domain as observed in other segments. Other key structural features of this segment include evidence for underthrust sediment, a shallower plate boundary decollement, and pervasive wedge-top slope failures (Fig. 11).

CASIE21 line PD14 represents the dominant structural style and seismic character within this segment (Fig. 11b). It is difficult to interpret subsurface structure in this profile due to the lack of coherent reflectivity, with seismic character ranging from semi-coherent near the toe of the wedge to mostly incoherent near the static backstop. The structural style is consistent throughout the accretionary wedge domain where seaward-verging thrust faults sole into a shallow plate boundary decollement with sediment underthrust beneath (Carbotte et al., 2024). The accretionary wedge in this segment is juxtaposed against the static backstop (Watt and Brothers, 2020) where the seismic character is incoherent and faults cannot be interpreted (Fig. 11b; light gray region). Bathymetric evidence does not provide evidence for continuous, major structural trends at

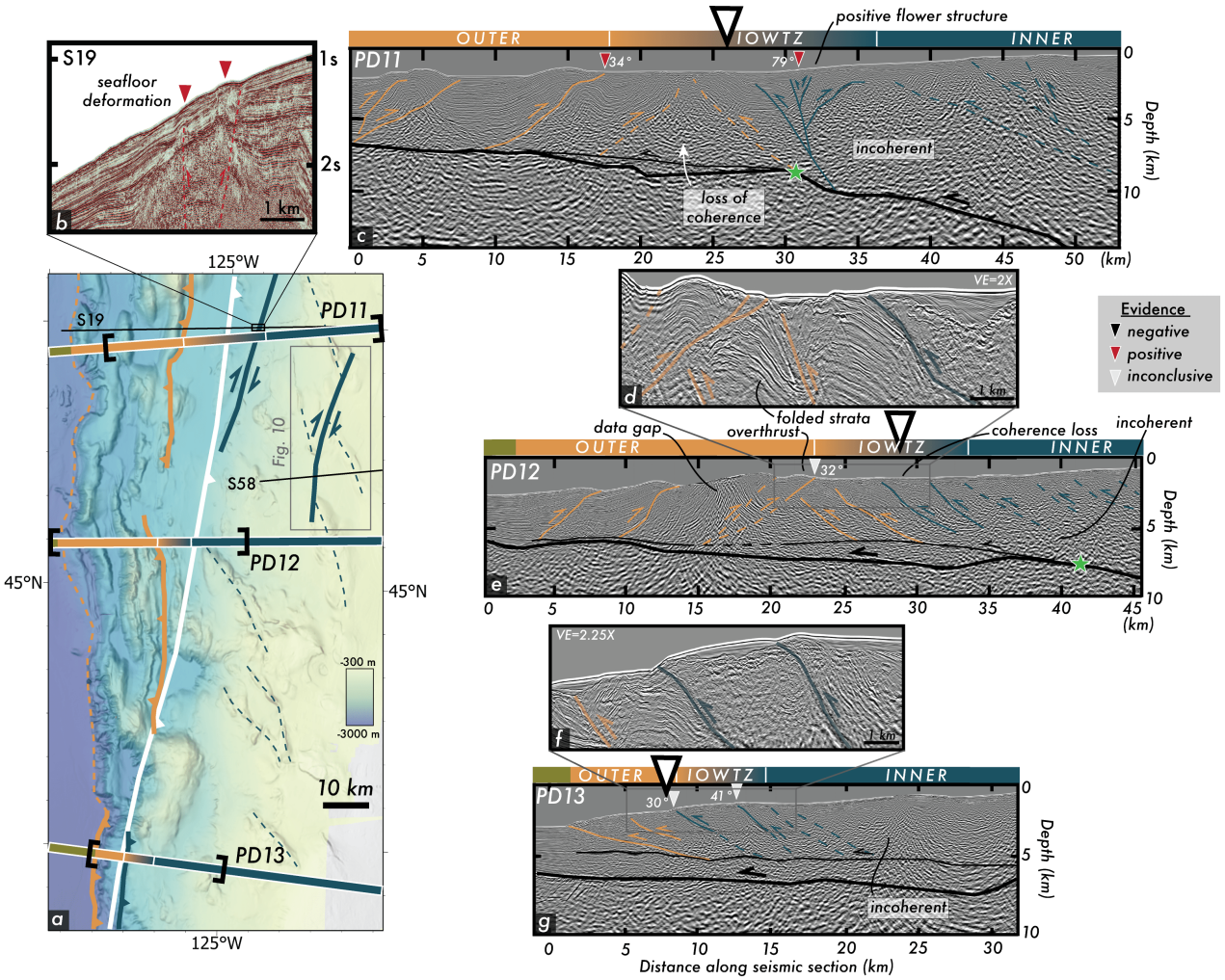

Figure 9 Tillamook subsegment of the Washington & Northern Oregon segment captured by PD11 to PD13 and USGS sparker seismic lines S19 and S58. Symbology is the same as Fig. 5. **a.** Map of 30-m USGS bathymetry showing seismic line locations and extent of wedge domains. Grey inset box shows region of Fig. 10. **b-g.** CASIE21 seismic lines PD11, PD12, and PD13 and USGS sparker seismic line S19.

the seafloor that can be traced along strike and linked to observed subsurface fault structure (Fig. 11a). Instead, the seafloor in this segment is chaotic, likely due to extensive slope failures in this region (e.g., Hill et al., 2022) that potentially disrupt the near-surface expression of wedge faulting (Fig. 11a,b). Fault structures identified in adjacent segments do not extend into this segment based on wedge structure and seafloor morphology.

3.5 Southern Oregon (~42-42.6°N)

The Southern Oregon segment is characterized by the re-emergence of an observable outer wedge domain (Fig. 12). The boundary between the Central and Southern Oregon segments also appears to correspond with the projected trace of the Blanco Transform Fault System (Fig. 3; BTFS). The Southern Oregon segment exhibits an indentation of the wedge between lines PD18 and PD19 corresponding with the Rogue Propagator Shear Zone (RPSZ) (Fig. 12a). North of this indentation in PD18, there is a narrow, ~5 km wide outer wedge composed of two imbricated seaward-verging thrust faults with mostly coherent reflectivity (Fig. 12c). Similar to faulting in the Central Oregon segment, these two outer wedge thrust faults are interpreted to sole into a shallower plate boundary decollement with sediment underthrust beneath (Carbotte et al., 2024). The IOWTZ in PD18 is ~7 km wide and composed of a single seaward-verging thrust sheet with mostly incoherent reflectivity (Fig. 12c). Within the inner wedge domain of PD18 it is difficult to interpret subsurface structure due to incoherent reflectivity. Some shallow fault structures are well-imaged; however, it is unclear how these structures sole into the subsurface. South of the wedge indentation, PD19 also exhibits a narrow ~5 km wide outer wedge characterized by 2-3 seaward-verging thrust sheets with coherent reflectivity that accrete the incoming sediment section (Fig. 12e). This differs from PD18 where sediment underthrusts beneath the outer wedge domain. The IOWTZ in PD19 is ~15 km wide and characterized by a structural gradient from mixed-verging thrust faulting to dominantly seaward-verging thrust faulting to the east. The observed structural gradient is accompanied by a gradient in the seismic character of the subsurface from mostly coherent to mostly incoherent reflectivity. The inner wedge domain in PD19 is characterized by incoherent reflectivity, which results in difficultly in interpreting subsurface structure

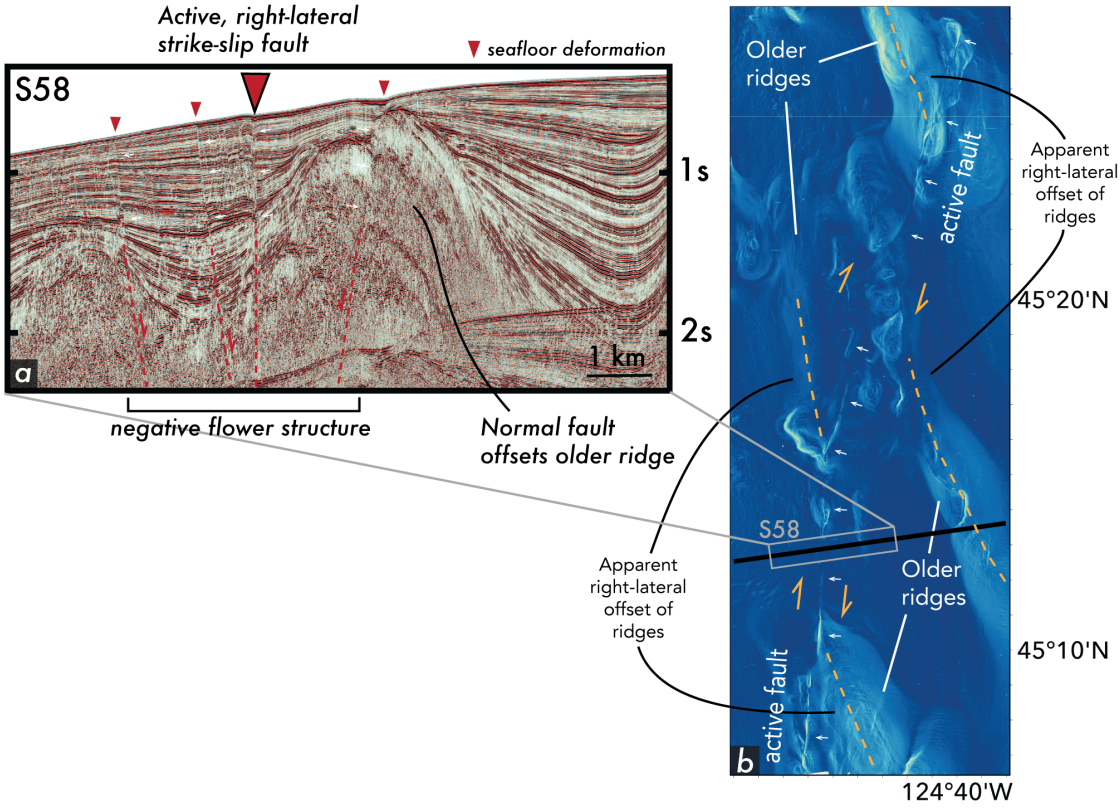

Figure 10 Active right-lateral strike-slip fault of the Tillamook subsegment. **a.** USGS sparker seismic line S58 showing evidence for an active right-lateral strike-slip fault. Surface displacements from subsidiary normal faults shown by small red arrows and are associated with subsurface fault denoted by red dotted lines. Large red arrow with black outline indicates the primary strike-slip fault scarp identified in the bathymetry. **b.** Multi-directional hillshade map created using USGS 30-m bathymetry showing younger fault scarp at seafloor (traced by small white arrows) cutting across older seafloor ridge structures. Lighter colors represent steeper slopes, darker colors represent shallower slopes. Fault trace accentuated by hillshaded map. Map extent denoted in Figure 9.

at greater depths.

PD18 captures a prominent seafloor ridge associated with a seaward-verging thrust fault at the IOWTZ with a dip of 29° (Fig. 12c). This fault appears to be inactive because it is buried by a basin of apparently flat-lying sediments and is associated with a seafloor slope failure (Fig. 12b). Therefore, its activity is classified as inconclusive due to a lack of higher resolution seismic imaging at this location (Fig. 12c). However, an adjacent outer wedge fault appears to tilt basin sediments and may be recently active, but this fault requires further investigation with near surface data (Fig. 12b). Other IOWTZ and inner faults imaged in PD18 are interpreted near the surface, but it is not clear if these faults are connected to the megathrust fault at depth due to a lack of coherent reflectivity (Fig. 12c).

In PD19, a landward-verging thrust fault at the IOWTZ is dipping at 38° (Fig. 12e). This fault appears to be overthrust onto an adjacent seaward-verging thrust fault, similar to the overthrust fault observed at the IOWTZ in PD12. This fault is a candidate out-of-sequence splay fault at the IOWTZ due to its apparent re-activation at the IOWTZ, connectivity with the megathrust fault at depth, and possible uplift of the seafloor (Fig. 12d). However, evidence for recent activity of this fault is inconclusive based on available data. Additionally, the length of this fault is only ~15 km and it is not connected to faulting north of the RPSZ based on its surface expression in the bathymetry and structural similarities with nearby faults in PD18 (Fig. 12a).

3.6 Summary of Results

Observations of IOWTZ structure, megasplay fault activity, outer wedge thrust fault vergence, and other key wedge structural features are used to define wedge segment boundaries (Table 1). Across the Northern and Central Vancouver Island segmentation boundary, thrust fault vergence of the outer wedge domain changes abruptly from landward to seaward, which appears to closely align with the Nootka Fault Zone (NFZ) (Rohr et al., 2018) (Figs. 3, 4, 5). A megasplay fault system is present along the Central Vancouver Island segment and has a prominent but discontinuous surface expression (Fig. 5). Between the Central Vancouver Island and Washington & Northern Oregon segments, the location of the segmentation boundary is uncertain due to a lack of seismic imaging between PD04 and PD05 (Fig. 3). This boundary may be gradational in nature due to the apparent lack of a major bounding structure, and therefore this area is defined as an ATZ at the segment boundary. The Washington & Northern Oregon segment is broadly defined by the extent of the wide outer wedge landward vergence zone that tapers at the north-

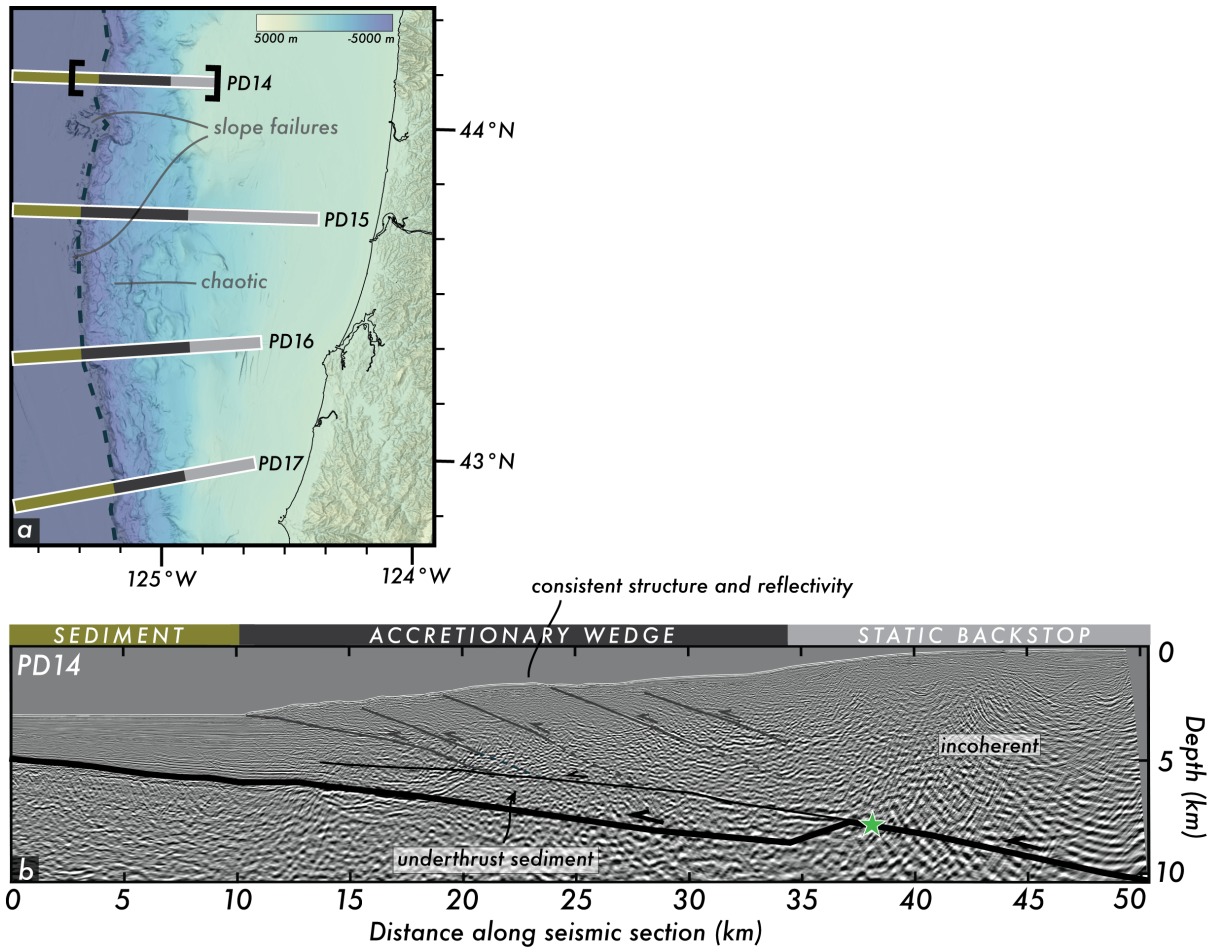

Figure 11 Central Oregon segment. **a.** Map of GMRT 50-m bathymetry showing location of line PD14. Symbology is the same as Fig. 5. **b.** CASIE21 seismic line PD14 with static backstop extent from Watt and Brothers (2020). Interpretation of underthrust sediment, plate hinge, and upper megathrust decollement from Carbotte et al. (2024).

ern and southern ends of the segment (Figs. 3, 4, 6-9). This segment is subdivided into three subsegments: Olympic (PD06-PD07), Astoria (PD08-PD09), Tillamook (PD10-PD12) based on transitions in faulting style and activity at the IOWTZ (Table 1). At the southern end of the Washington & Northern Oregon segment, there is an ATZ in PD13 where there is an outer wedge domain and underthrust sediment beneath the wedge, both key structural features of adjacent segments (Fig. 9). In the Central Oregon segment, no clear inner or outer wedge domains can be identified within the wedge (Fig. 11). Instead, there is a consistent structural style and seismic character throughout the entire accretionary wedge distinctly characterized by underthrust sediment and extensive wedge-top slope failures. In the Southern Oregon segment, a narrow outer wedge domain and corresponding IOWTZ re-emerges that is aligned with the projected location of the Blanco Transform Fault System (BTFS) (Ren et al., 2023) and this segment is dissected by the Rogue Propagator Shear Zone (RPSZ) (Figs. 3, 12). An ATZ is defined between the BTFS and RPSZ at the location of PD18 in which underthrust sediment and a clear outer wedge domain is observed, which are key features of both the adjacent Central and Southern Oregon segments (Table 1). Overall, there are observable changes in wedge structure and faulting over relatively short along-strike distances (10s of kms), which enables clear delineation of regional-scale segmentation boundaries within the Cascadia accretionary wedge.

4 Discussion

4.1 Impact of wedge sedimentation on megasplay fault structural evolution and activity

Sedimentation onto the Cascadia accretionary wedge during the Pleistocene likely plays a major role in the wedge structural evolution and modern-day wedge structure. We suggest that variations in sedimentation onto the wedge along strike significantly contribute to the apparent segmentation of megasplay fault development and activity at the IOWTZ.

The rapid growth of the outer wedge domain in the Washington & Northern Oregon segment is thought to have begun at roughly 1.5 Ma during the early Pleistocene when large quantities of glacial sediment were deposited onto the offshore accretionary wedge (Flueh et al., 1998). Due to lower sea levels during Pleistocene glaciation, sediments were able to bypass the continental shelf, flow into submarine channels, and deposit directly atop the Cascadia accretionary wedge (Clark et al., 2014; Klotsko et al., 2021). This process formed the Astoria and Nitinat sedimentary fans which blanket

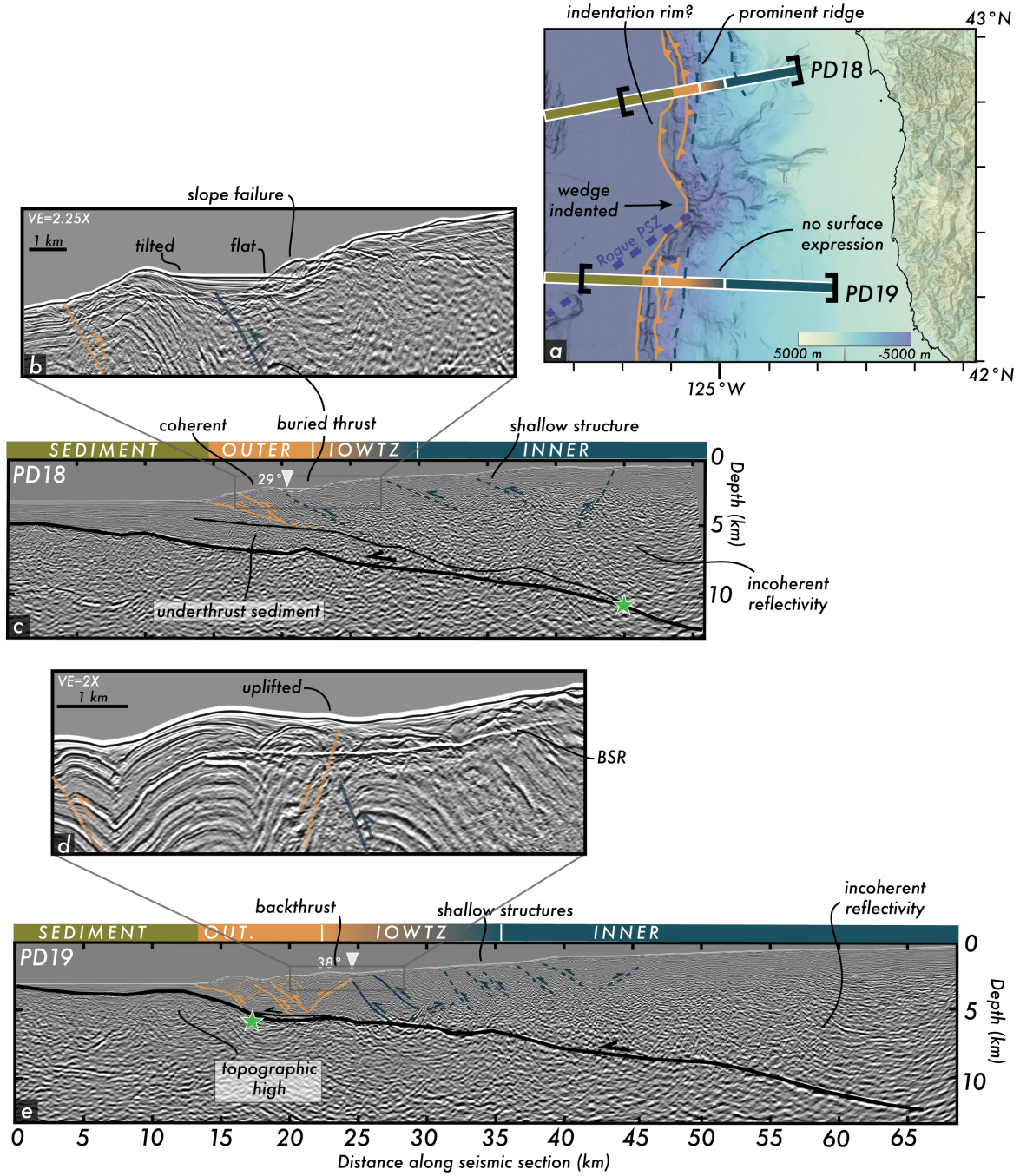

Figure 12 Southern Oregon segment. Symbology is the same as Figure 5. **a.** Map of GMRT 50-m bathymetry showing locations of lines PD18 and PD19. **b-c.** CASIE21 seismic lines PD18 and PD19.

the outer wedge region for the Washington & Northern Oregon segment (Underwood, 2002).

During the Miocene, prior to glacial sedimentation, we hypothesize that the wedge was in steady-state deformation, maintaining critical taper through sediment subduction and the addition of incoming sediment through accretion via seaward verging thrust faults and underplating (Dahlen, 1990) (Fig. 13a). It has been suggested that rapid outward growth of the wedge likely occurred in response to heavy influx of sediment resulting from glacial sedimentation of the central Cascadia region beginning in the Pleistocene (Adam et al., 2004; Simpson, 2010). This growth formed the modern-day inner-outer wedge boundary (i.e., IOWTZ) between the older, more deformed Miocene wedge and the younger, less deformed Pleistocene wedge (Fig. 13b). The rapid addition of new material to the wedge would result in the overall deformational style of the wedge to transition from a steady-state to wedge-taper disequilibrium. The presence of disequilibrium structures during heavy sedimentation is predicted by mechanical models, which includes observations of buried structures, reduced wedge surface slopes, widespread wedge top basins, and increased thrust spacing (Simpson, 2010). We observe many of these disequilibrium features throughout the outer wedge domain of the Washington & Northern Oregon segment (Figs. 3, 6-9). Numerical models also show that when a stress barrier is present in the wedge, megathrust rupture tends to propagate up splay faults at this barrier (Wendt et al., 2009).

Segment name and latitudinal extent		CASIE21 lines	IOWTZ structure	Megasplay fault activity	Outer wedge thrust fault vergence	Key wedge structural features
Northern Vancouver Island (49.2–49.6°N)		PD02	Relatively undeformed, possible megasplay structure	N/A	Landward	Landward vergence, possible slab tear
Central Vancouver Island (48.3–49.2°N)		PD03-04	Megasplay fault system with prominent but discontinuous surface expression	Inconclusive	Seaward	Near-identical frontal thrust structure, megasplay faults
Washington and Northern Oregon (44.2–48.3°N)	Olympic (48.3–47°N)	PD06-07	Megasplay faults buried by 1–2 km thick sediment	Negative	Landward-dominated mixed	Extensive and wide landward vergence zone
	Astoria (47–45.8°N)	PD08-09	Megasplay fault with prominent and continuous surface expression	Inconclusive to negative		
	Tillamook (45.8–44.2°N)	PD10-12	Active strike-slip and splay faults present at or near IOWTZ	N/A		
Central Oregon (42.6–44.2°N)		PD14-17	N/A	N/A	N/A	Underthrust sediment, wedge-top slope failures, no outer wedge/IOWTZ domain
Southern Oregon (42–42.6°N)		PD18-19	Possible megasplay fault structures	Inconclusive	Seaward-dominated mixed	Re-emergent outer wedge/IOWTZ domains

Table 1 Structural features used to define each along-strike accretionary wedge segment and subsegment. "N/A" indicates category is "not applicable" for given segment.

The formation of the boundary between the inner and outer wedge during the Pleistocene created a major stress barrier in the wedge between the younger, less deformed, and therefore weaker Pleistocene wedge; and older, more deformed, and therefore stronger Miocene wedge. This is likely the mechanism for the development of out-of-sequence megasplay faults at the IOWTZ throughout the Washington & Northern Oregon segment (Fig. 13c), despite the lack of evidence for recent activity on these faults (Fig. 14).

The rate and location of syntectonic sedimentation of accretionary wedges directly affects out-of-sequence megasplay fault evolution and activity (Strasser et al., 2009; Simpson, 2010; Mannu et al., 2016). Numerical models and real-world observations from these studies show that rapid sedimentation on the wedge can bury and deactivate out-of-sequence megasplay faults. Evidence that megasplay faults were once active is observed at the IOWTZ in PD06, PD07, PD09, and PD10 (Figs. 6-7); however, these megasplay fault structures are now buried by undeformed sediment and do not show evidence for late Quaternary activity (Fig. 13d). Deactivation of out-of-sequence faults due to high sedimentation rates has also been observed within Alaska, Makran, and Nankai accretionary wedges (e.g., Strasser et al., 2009; Mannu et al., 2016). The location of the potentially active megasplay fault structure at the IOWTZ captured by PD08 may have experienced lower sedimentation rates than surrounding areas, resulting in sustained activity and uplift of this megasplay fault structure (Fig. 13e). Numerical models by Simpson (2010) and Mannu et al. (2016), along with observations from the Nankai accretionary wedge by Strasser et al. (2009), show that higher sedimentation rates correlate with faster seaward migration of the deformation front, and therefore, a more rapid growth of the outer wedge and reduced activity on out-of-sequence thrusts (Fig. 13d). Since the outer wedge in PD08 is narrower compared to the outer wedge to the north and south, this provides further evidence that sedimentation rates may have been lower in this location. Additionally, the active domain of the outer wedge, as defined by Ledeczi et al. (2024), appears to narrow in the vicinity of PD08, supporting the conclusion of decreased frontal accretion in this location, with a preference for uplift on the identified out-of-sequence megasplay fault system (Fig. 8). Submarine channels also appear to be routed around the convex-outward, bathymetric high corresponding with this megasplay fault system in PD08 (Figs. 8, 14). This indicates that the rate of megasplay fault uplift likely exceeds the rate of channel incision in this location, effectively routing sediments away from this structural high and further reducing sedimentation rates and sediment burial of this structure. The routing of sediment away from this structural high may have created a deformation-sedimentation feedback loop (Noda et al., 2020; McArthur et al., 2021) that promotes continued uplift on this fault. These findings showcase an important interplay between the surface processes of submarine channels, sedimentation rates, and fault-related uplift rates that controls whether an out-of-sequence fault remains active or becomes inac-

tive. However, it is important to note that the mechanical response of the wedge to sedimentation is not immediate, and that response time depends on sedimentation rate (e.g., Mannu et al., 2016). This is a particularly important consideration in determining whether faults are still deforming based on observations of modern-day wedge structure, as wedge deformation requires time to respond to sedimentation or a lack thereof. In PD11 and PD12, the outer wedge is narrow compared to areas further north and there is no evidence for a megasplay fault structure in this region (Fig. 9). This suggests that a megasplay fault did not activate in this region because of lower relative sedimentation rates that resulted in a narrower outer wedge. Due to the narrow outer wedge in this region, there is consequently a less effective stress barrier created between the inner and outer wedge, inhibiting the activation of out-of-sequence faulting at the IOWTZ.

Other regions of the Cascadia margin did not experience the same levels of glacial sediment deposition as compared to Washington & Northern Oregon segment; therefore, a wide outer wedge did not form in these regions. In the Northern & Central Vancouver Island segments captured by PD03 and PD04, a narrow outer wedge is observed. This narrow wedge is not sufficient in creating a stress barrier necessary that would promote megasplay fault rupture. Similarly, in the Central Oregon segment, clear inner or outer wedge domains cannot be distinguished based on seismic character and structural style (Fig. 11). This indicates that there was only modest accretion of sediments during the Pleistocene in this region and hence no stress barrier was created between the inner and outer wedge that would result in the development of an out-of-sequence megasplay fault system as observed in the Washington & Northern Oregon segment. The wedge in this segment likely resembles the Miocene wedge prior to accretion of the wide outer wedge domain in the Washington & Northern Oregon segment during the Pleistocene and may be akin to the modern-day inner wedge of adjacent regions. This conclusion is further supported by the similarity in structure between the modern wedge of the Central Oregon segment and the inner wedge domain of other segments along strike, which is characterized by a series of imbricated, seaward-verging thrust faults and mostly incoherent seismic character.

4.2 Influence of subducting topography on accretionary wedge evolution

We suggest that the development of an outer wedge domain and activation of megasplay faults at the IOWTZ in the Northern and Central Vancouver Island segments and the Southern Oregon segment may be controlled by subducting topography on the downgoing plate. Analogue sandbox experiments show that seamount subduction can result in the outward growth of the wedge and development of out-of-sequence thrust faults between the older and younger wedge domains (Dominguez et al., 2000). The subduction of local topography offshore the Vancouver Island and Southern Oregon regions associated with propagator wakes and shear zones on the downgoing plate (Wilson, 2002; Nedimović et al., 2009; Hutchinson et al., 2023; Carbotte et al., 2024) may provide a mechanism for the outward growth of the wedge in these regions that does not require the same levels of glacial sedimentation as suggested for the formation of the wide outer wedge domain in the Washington & Northern Oregon segment. Dominguez et al. (2000) show out-of-sequence faults are observed to form in the older, more cohesive domain of the wedge. As predicted by Dominguez et al. (2000), out-of-sequence megasplay faulting associated with subducting topography, observed in PD03 and PD04, primarily occurs within the more cohesive inner wedge domain at the IOWTZ (Fig. 5). In PD04, the development of out-of-sequence, megasplay faults at the IOWTZ is co-located with rough subducting topography of a propagator shear zone (Fig. 5c). In PD03, although significant topography is not observed on the downgoing plate at the IOWTZ (Fig. 5b), this line is located along the indentation rim of the "shadow zone" that likely formed due to subducting topography captured in PD02 (Fig. 5a). Modeling of seamount subduction from Dominguez et al. (2000) shows that the rim of the shadow zone will also exhibit out-of-sequence megasplay fault activation at the IOWTZ in addition to the location where the local topography itself is being subducted. There is not sufficient seismic and bathymetric evidence to conclusively determine whether there is active megasplay faulting in PD02; however, out-of-sequence splay faulting is likely present in this area and evolving in response to the regional subduction of the topography. Similar to how the wedge responds to sedimentation loads, the wedge structure may require time to respond to the subduction of lower plate topography.

At the Southern Oregon segment, topography associated with the RPSZ is subducting beneath the wedge (Chaytor et al., 2004; Carbotte et al., 2024). It is also important to consider that, at longer topographic wavelengths, the more buoyant crust of the Gorda plate is subducting in this region along with shorter wavelength topography associated with the RPSZ. In the Southern Oregon segment, the re-emergence of an outer wedge domain and an ATZ is observed in PD18 that defines the segment boundary between Central and Southern Oregon (Figs. 3, 12). Subducting topography is not associated with the formation of the outer wedge domain in PD18 (Fig. 12b), but the formation of the outer wedge in PD18 could be due to a similar "indentation rim" process as suggested for PD03 (Fig. 5). This formation may also be due to longer wavelength topography associated with the Gorda plate. The local re-emergence of an outer wedge domain might also be due to a gradational response in wedge structural style across a major segmentation boundary in the wedge at the ATZ in the region of PD18. In PD19, a major topographic high is observed at the deformation front which appears to be in an initial stage of subduction beneath the wedge (Fig. 12c). Dominguez et al. (2000) show that in addition to the development of an outer wedge, prominent backthrusts will also develop at this early stage of seamount subduction. In PD19, a landward verging backthrust dipping at 38° is observed (Fig. 12c; white arrow), consistent with

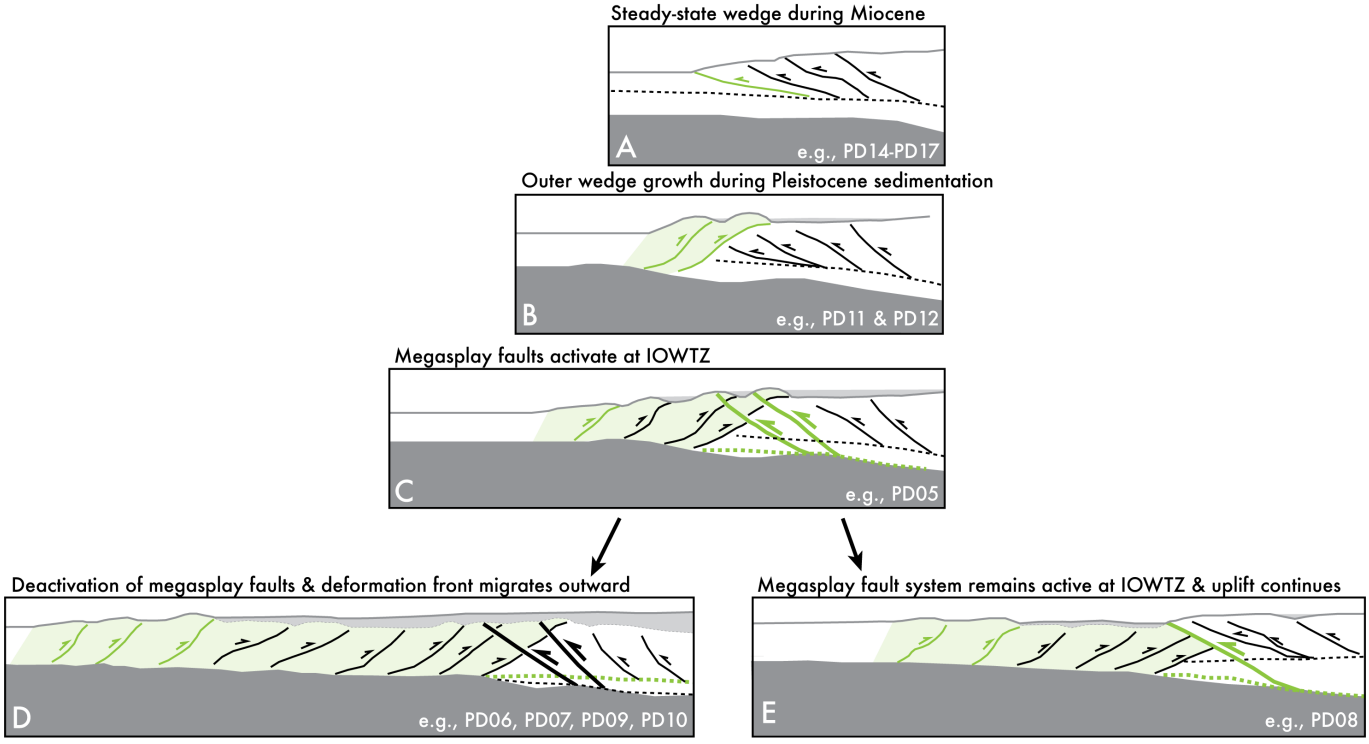

Figure 13 Schematic figure showing a simplified representation of the development and evolution of megasplay faulting in Cascadia. **A-E.** Simplified diagrams based on observed accretionary wedge illustrating the hypothesis for how megasplay faulting would develop and remain active or become inactive due to sedimentation. Green lines represent active structures, and black lines represent inactive structures. White domains represent the inner wedge, and green domains represent the outer wedge. Seismic lines that were used to develop the diagrams are noted in the lower left corner of each picture. Bolded lines show megasplay faults. Dotted lines represent decollements above top of crust. Solid gray represents the Juan de Fuca plate.

this prediction. Dominguez et al. (2000) find that major out-of-sequence thrust faults due to subduction of topography do not appear to develop until later stages of seamount subduction. This could demonstrate how subducting topography in this location may have been sufficient to spur the development of an outer wedge domain and backthrusts, but not yet have led to the full activation and development of megasplay fault structures as is observed in the Central Vancouver Island segment. This could indicate that out-of-sequence faults may develop in this location in the future over the course of outer wedge development and seamount subduction on a longer timescale.

4.3 Linking accretionary wedge structure with proposed segmentation of the Cascadia Subduction Zone

Variability in accretionary wedge structure and morphology at convergent plate boundaries has been linked to segmentation of lower plate structure and megathrust fault behavior (Kopp, 2013; Cook et al., 2014; McNeill and Henstock, 2014). Here we aim to link our observations of accretionary wedge structure and megasplay fault activity at the IOWTZ to prior observations for segmentation of the Cascadia subduction zone based on subducting plate structure (Carbotte et al., 2024) and morphotectonic variability (Watt and Brothers, 2020).

At the Nootka Fault Zone, Carbotte et al. (2024) found that the downgoing plate is deeper and more steeply dipping compared to surroundings. To the east of the Nootka Fault Zone, they observe a relatively shallower downgoing plate dip near the deformation front, delineating a clear segmentation boundary in lower plate structure. This segmentation in lower plate structure at the Nootka Fault Zone was previously linked to a structural and morphologic transition in the accretionary wedge, with a sharp bend observed in the overall trend of the deformation front (Watt and Brothers, 2020). This fault-controlled segmentation boundary is linked to a clear transition in outer wedge structural style from dominantly landward-verging thrust faulting in the Northern Vancouver Island segment to mixed-seaward-verging thrust faulting in the Central Vancouver Island segment (Fig. 5, Table 1). Additionally, megasplay fault structures observed at the IOWTZ in CASIE21 lines PD03 and PD04 do not connect across this segmentation boundary (Fig. 14).

At ~47°N, and the boundary between the Olympic and Astoria subsegments, the North and South Nitinat strike-slip faults cross the deformation front and are expressed in both the upper and lower plate (Goldfinger et al., 1997) (Fig. 14). Using CASIE21 seismic profiles, Carbotte et al. (2024) find these faults to extend across the margin beneath the continental shelf where

the fault system offsets basement rock by over 1 km. These faults are found to be coincident with a seaward step in the Siletz terrane and a local seaward step in the location of the dynamic backstop from Watt and Brothers (2020) (refer to "dynamic backstop" in Fig. 1). At the location where these faults cut across the wedge, there is evidence in CASIE21 line PD08 for a potentially active megasplay fault zone associated with a sharp and distinctively convex-outward boundary between the inner and outer wedge domains (Fig. 8). The location of this fault system is associated with an increase in seafloor elevation, a steepening of the downgoing plate dip (refer to "plate hinge" in Fig. 8), and a shallowing of the plate boundary decollement (Fig. 8). We propose that subducting topography in the lower plate related to the North and South Nitinat strike-slip faults is linked to the localized activity and uplift of this megasplay fault structure at the IOWTZ. This hypothesis is further supported by the presence of active listric normal faults in the upper slope of the margin in this region (Figs. 7b, 8a) (McNeill et al., 1997; Watt and Brothers, 2020) that could potentially be the result of extensional collapse within the hanging wall of the megasplay fault system due to subducting topography and associated fault uplift. A similar process has been observed at the Hikurangi subduction zone where relief on the subducted Pacific plate has been linked to out-of-sequence activity of the Lachlan thrust fault system and subsequent development of listric normal faults (Barnes et al., 2002).

Shallowly dipping inner wedge thrust faults appear to sole into a shallower decollement within the hanging wall of the proposed megasplay fault system (Fig. 8b). This further implies that preferential uplift has occurred on this megasplay fault structure at the IOWTZ and that uplifted inner wedge material has been underplated to the base of the wedge (Fig. 13e). An alternative explanation could be that these shallowly dipping faults developed within the upper plate along an upper-level decollement. However, these faults are not associated with significant topography at the seafloor that would suggest that this occurred (Fig. 8b). A similar process to that proposed for PD08 has also been observed at the north Ecuador-south Colombia subduction margin where sediment underplating to the base of the inner wedge is associated with out-of-sequence activation of splay faults at the inner-outer wedge boundary and broad uplift of the inner wedge domain through slip on this splay fault system over multiple earthquake cycles (Collot et al., 2008).

Between 46.5°N and 44.5°N, there is a marked change in the lower plate geometry characterized by a steepening of the downgoing plate dip (Carbotte et al., 2024). The width of the outer wedge narrows southward through this region, starting near the boundary between Watt and Brothers (2020) morphotectonic regions 2 & 3 and the Willapa Canyon Fault Zone, until the boundary between the Washington & Northern Oregon and Central Oregon segments. South of this apparent segmentation boundary, starting at PD10, faulting style at the IOWTZ is observed to change from compressional to transform moving south along the margin (Figs. 7, 14). This change in faulting style at the IOWTZ defines the Tillamook subsegment boundary from PD10-12 within this segment (Table 1). South of PD10, a megasplay fault style structure is not present at the IOWTZ. At the location of the Wecoma Fault and the secondary morphotectonic segment boundary from Watt and Brothers (2020) (Fig. 14; purple dotted line), the outer wedge domain increasingly narrows and thrust fault vergence changes from dominantly landward-verging to seaward-verging and strike slip-fault activity appears to cease through this region until the ATZ captured by PD13 (Figs. 3, 7, 14, Table 1). This may illustrate a potential mechanical tradeoff between margin-parallel and margin-perpendicular strike-slip faults in the accommodation of shear strain related to oblique convergence in this region. Overall, we suggest that segmentation due to lower plate faults likely exerts a primary control on megasplay and other out-of-sequence splay fault activity within the accretionary wedge of this region and overall wedge morphology.

In some locations along the margin, the IOWTZ corresponds to the position of a gradual to sharp increase in the dip of the downgoing Juan de Fuca plate, or plate hinge (Figs. 5-9, 11, 12). In particular, for CASIE21 lines where active out-of-sequence faulting is observed within the IOWTZ, the plate hinge is located near the base of these faults (e.g., PD08, PD10, PD11). This spatial relationship suggests that variations in accretionary wedge structure and geology are directly related to variations in the dip of the downgoing plate. However, the underlying processes controlling this proposed relationship are yet to be determined. Carbotte et al. (2024) suggests that, due to the weak, warm and hence buoyant nature of the Juan de Fuca plate related to its relatively young age, lower plate bending may be more sensitive to change in the strength and density of the overlying plate such as the transition from the younger outer to older inner wedge domains. Accretionary wedge faulting likely also responds to changes in the dip of the downgoing plate because the change in plate dip could effectively act as a stress barrier to the propagation of megathrust slip towards the trench. Recent numerical modeling of megathrust fault ruptures has shown that fault dip and curvature are primary controls on rupture propagation and segmentation as well as earthquake recurrence rates (Biemiller et al., 2024). Therefore, the observed change in plate dip and high curvature at the plate hinge location could potentially promote megasplay fault activation at the IOWTZ.

4.4 Re-evaluation of splay fault rupture scenarios for Cascadia and implications for future hazard modeling

Prior to this study, it had been widely proposed (or assumed) that an active megasplay fault exists at the IOWTZ in Cascadia spanning continuously from Vancouver Island to Oregon (e.g., Priest et al., 2009; Witter et al., 2013; Gao et al., 2018; Sypus, 2019; Lotto et al., 2018). Earthquake and tsunami hazard assessments developed from simulated rupture on this hypothetical fault, specifically the L1 splay fault scenario,

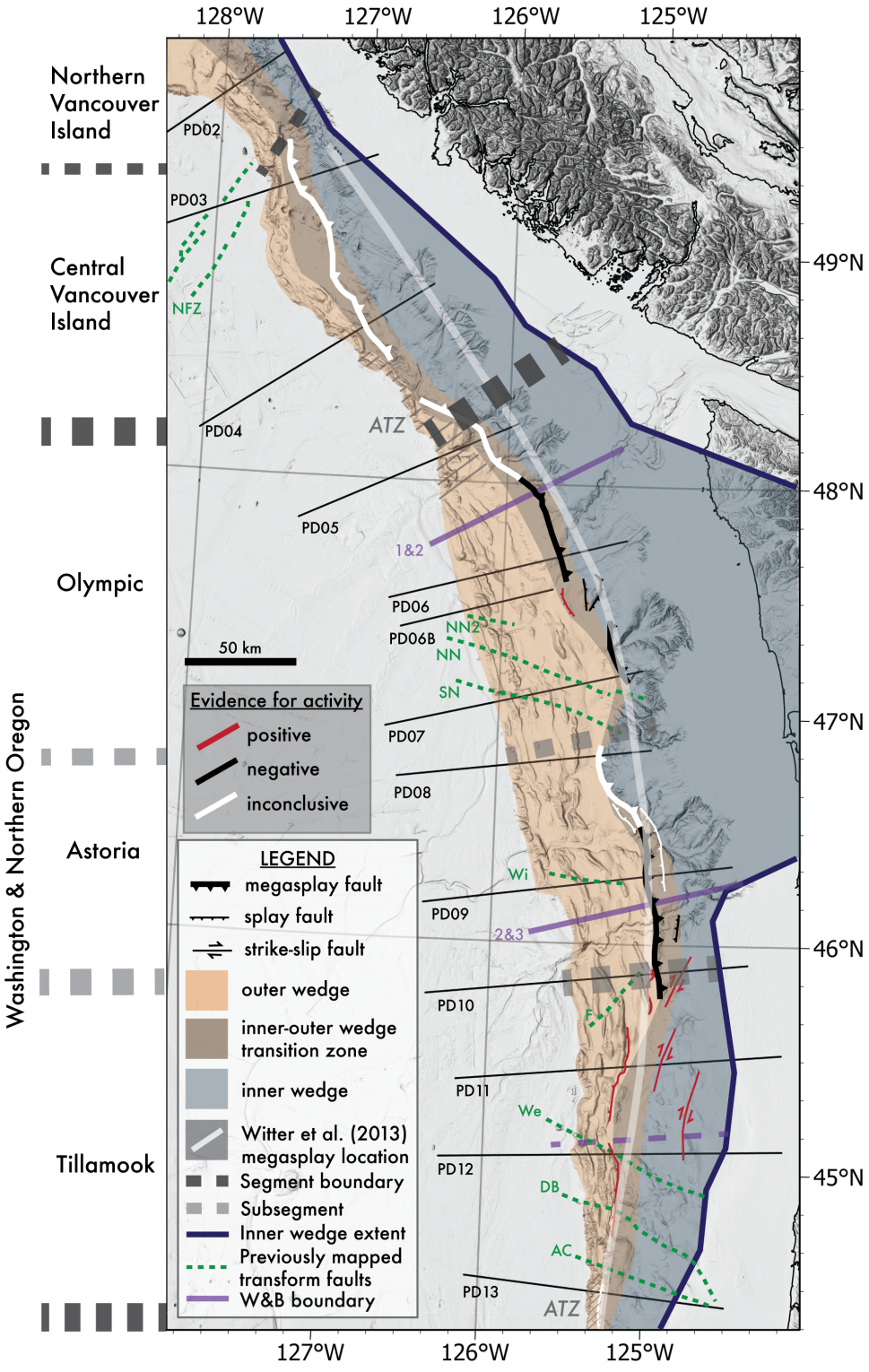

Figure 14 Map showing extent of inner (blue) and outer (orange) wedge domains in the accretionary wedge and the transition zone (blueish orange) between these domains as determined using CASIE21 seismic reflection images. These domains correspond with domains identified in seismic cross-sections shown in Figure 3. Splay faults at the IOWTZ are shown. Bold faults represent megasplay faults in this zone and non-bolded faults represent splay faults. Strike slip faults are represented with dotted lines. Different colors represent our analysis of fault activity: red indicates faults with positive evidence of late Quaternary activity, black indicates faults with negative evidence of late Quaternary activity, and white indicates inconclusive evidence for late Quaternary activity given our analysis of current datasets (this study, Ledeczi et al., 2024).

have been routinely included in models underlying numerous hazard assessments for the Cascadia region (e.g., Lee, 2017; Morkner, 2019; Dolcimascolo et al., 2022; La Selle et al., 2024; Bernard, 2022). Using new CASIE21 MCS and USGS sparker seismic profiles along with GMRT 50-m and USGS 30-m bathymetry compilations, the IOWTZ between the inner and outer wedge domains was located and fault structure was analyzed in this zone from Vancouver Island to Oregon. Results indicate there is not sufficient evidence to support the hypothesis for an active, through-going megasplay fault system at the IOWTZ along the Cascadia subduction zone margin spanning the region between latitudes 44° and 50°N. Instead, megasplay fault structure and activity in Cascadia is highly variable and segmented along strike. Furthermore, positive or inconclusive evidence of a recently active major out-of-sequence splay fault is only present in a few isolated regions along strike at the IOWTZ (Fig. 14). This has major implications for the likelihood of the L1 and other megasplay scenarios as a significant tsunami source (e.g., Witter et al., 2013).

Synthesizing our results, a map of simplified megasplay fault structure and activity at or near the IOWTZ is presented, focused on the region of the previously proposed active, margin-spanning megasplay fault from Witter et al. (2013) (Fig. 14). Through joint analysis of multiple marine geophysical datasets, most megasplay fault structures at the IOWTZ are discovered to either have inconclusive or negative evidence for recent activity. Therefore, it is unlikely that the L1 scenario represents plausible future Cascadia megathrust earthquakes, except in some strike-limited locations. This result demonstrates how comprehensive, high-resolution seismic surveying and seafloor mapping of the Cascadia accretionary wedge can help clarify how faults connect through space between seismic lines and characterize the expression of active faulting at the seafloor. More comprehensive surveying and mapping could ultimately improve our understanding of which faults have slipped in past Cascadia earthquakes and which faults might slip in future earthquakes. Such work is crucial for accurately quantifying tsunami hazard and risk along the Pacific Northwest coast.

Incorporating the segmented nature of accretionary wedge splay faulting at the IOWTZ into modeling efforts could help quantify earthquake and tsunami hazards at the Cascadia subduction zone. Regional scenarios could include different styles and locations of splay fault rupture. In the Central Vancouver Island segment between latitudes 48° and 49.5°N, megasplay fault rupture on a system of seaward-verging thrust faults with an average dip of ~40° is likely at the IOWTZ in addition to frontal thrust rupture (Figs. 5, 14). In the Washington & Northern Oregon segment, rupture on multiple splay faults at the toe of the wedge near the deformation front should be primarily examined based on evidence for late Quaternary activity of splay faults (Ledeczi et al., 2024). Localized scenarios could also be modeled, including rupture on an isolated seaward-verging megasplay fault dipping at ~30° as identified in CASIE21 line PD08 in the region offshore Grays Harbor, Washington between 46.5° and 47°N (Figs. 7, 8, 14), or rupture on the system of active right-lateral strike-slip faults identified in CASIE21 lines PD10, PD11, and PD12 between 45° and 46°N spanning roughly from Seaside to Newport, Oregon (Figs. 9, 14).

5 Conclusions

Overall, although megasplay fault structures exist and may be locally active at the IOWTZ in a few locations along strike, we find that there is not sufficient evidence supporting the previously proposed hypothesis for an active, margin-spanning megasplay fault system in Cascadia (e.g., Witter et al., 2013). Instead, the structure and activity of faulting at the IOWTZ is highly variable and segmented along-strike, consistent with the segmentation of other physical and mechanical properties at the Cascadia subduction zone (Underwood, 2002; Adam et al., 2004; Han et al., 2018; Watt and Brothers, 2020; Walton et al., 2021; Carbotte et al., 2024; Booth-Rea et al., 2008). Megasplay fault formation and segmentation is controlled by numerous factors, including margin lithology and strength, wedge sedimentation, sediment accretion, subducting topography, and changes in downgoing plate dip. The substantial variations in megasplay fault structure and activity along-strike presented in this study have important implications for earthquake and tsunami hazard at the Cascadia subduction zone. Through our comprehensive analysis of the CASIE21 and USGS sparker seismic reflection profiles along with the best available resolution of bathymetry, we conclude:

- There is no evidence to support the previously proposed hypothesis for an active, margin-spanning megasplay fault system at the IOWTZ in Cascadia.
- Megasplay fault structures exist but are only locally active at the IOWTZ at a few, relatively isolated locations along strike.
- Sedimentation onto the wedge surface likely plays a primary role in megasplay fault activation (or lack thereof) and evolution at the Cascadia subduction zone, while subducting topography may also influence out-of-sequence faulting in specific, relatively localized regions.
- Segmentation of downgoing plate structure and morphology is closely linked to the observed variations in upper-plate architecture and faulting at the IOWTZ.
- Future modeling studies for Cascadia could incorporate megasplay fault location, geometry, and activity as presented in this study.

Acknowledgements

This work was supported by funding from the University of Washington and National Science Foundation awards 2103713 and 2217468. We gratefully acknowledge the Cascadia Coastlines and Peoples (CoPes) Hub and the CASIE21 Science Team, both which provided a

community and environment to inspire, motivate, and foster the completion of this project. Thank you to the crew on the MGL2104 expedition who assisted in the collection of the CASIE21 seismic data. We further acknowledge Ryuta Arai, Jared Kluesner, and two anonymous reviewers for their constructive and thorough reviews that greatly improved the quality of this manuscript. Madeleine would also like to specially thank Tamara Aránguiz-Rago and Kimberly Sinclair for their constant support throughout the preparation of this manuscript. Any use of trade, firm, or product names is for description purposes only and does not imply endorsement by the U.S. Government.

Data and Code Availability Statement

Geophysical data used in the study are currently publicly available. CASIE21 seismic data are available on the *Marine Geoscience Data System* (Carbotte et al., 2023). High-resolution multi-channel sparker seismic data can be found in a USGS data release (Balster-Gee et al., 2023, USGS field activity 2019-024-FA). Global Multi-Resolution Topography (Ryan et al., 2009) can be downloaded at www.gmrt.org. USGS 30-m bathymetry data are available in a USGS data release (Dartnell et al., 2021, 2023). *Kingdom Suite* software was used for interpretation of all seismic data. Interpretation of bathymetric data and development of all maps and figures was completed in *ArcGIS Pro* and *Adobe Illustrator*.

Competing interests

The authors have no competing interests.

References

Adam, J., Klaeschen, D., Kukowski, N., and Flueh, E. Upward delamination of Cascadia Basin sediment infill with landward frontal accretion thrusting caused by rapid glacial age material flux. *Tectonics*, 23(3), June 2004. doi: 10.1029/2002tc001475.

Aslam, K. S., Thomas, A. M., and Melgar, D. The Effect of Fore-Arc Deformation on Shallow Earthquake Rupture Behavior in the Cascadia Subduction Zone. *Geophysical Research Letters*, 48 (20), Oct. 2021. doi: 10.1029/2021gl093941.

Baba, T. and Cummins, P. R. Contiguous rupture areas of two Nankai Trough earthquakes revealed by high-resolution tsunami waveform inversion. *Geophysical Research Letters*, 32 (8), Apr. 2005. doi: 10.1029/2004gl022320.

Balster-Gee, A. F., Miller, N. C., Watt, J. T., Roland, E. C., Kluesner, J. W., Heller, S. J., Hart, P. E., Sliter, R. W., Myers, E. K., Wyland, R. M., Marcuson, R. K., Johnson, C., Nichols, A. R., Pszczola, K., and Williams, C. High-resolution multichannel sparker seismic-reflection and chirp sub-bottom data acquired along the Cascadia margin during USGS field activity 2019-024-FA [dataset], 2023. doi: 10.5066/P96ZBXK8.

Barnes, P. M., Nicol, A., and Harrison, T. Late Cenozoic evolution and earthquake potential of an active listric thrust complex above the Hikurangi subduction zone, New Zealand. *Geological Society of America Bulletin*, 114(11):1379–1405, Nov. 2002. doi: 10.1130/0016-7606(2002)114<1379:lceaep>2.0.co;2.

Bernard, E. N. Tsunami Preparedness: Is Zero Casualties Possible? *Pure and Applied Geophysics*, 180(5):1573–1586, Jan. 2022. doi: 10.1007/s00024-022-02948-7.

Berndt, C., Bünz, S., Clayton, T., Mienert, J., and Saunders, M. Seismic character of bottom simulating reflectors: examples from the mid-Norwegian margin. *Marine and Petroleum Geology*, 21 (6):723–733, June 2004. doi: 10.1016/j.marpetgeo.2004.02.003.

Biemiller, J., Gabriel, A., May, D. A., and Staisch, L. Subduction Zone Geometry Modulates the Megathrust Earthquake Cycle: Magnitude, Recurrence, and Variability. *Journal of Geophysical Research: Solid Earth*, 129(8), Aug. 2024. doi: 10.1029/2024jb029191.

Booth-Rea, G., Klaeschen, D., Grevemeyer, I., and Reston, T. Heterogeneous deformation in the Cascadia convergent margin and its relation to thermal gradient (Washington, NW USA). *Tectonics*, 27(4), July 2008. doi: 10.1029/2007tc002209.

Breen, N. A., Silver, E. A., and Hussong, D. M. Structural styles of an accretionary wedge south of the island of Sumba, Indonesia, revealed by SeaMARC II side scan sonar. *Geological Society of America Bulletin*, 97(10):1250, 1986. doi: 10.1130/0016-7606(1986)97<1250:ssoaaw>2.0.co;2.

Byrne, D., Wang, W., and Davis, D. Mechanical role of backstops in the growth of forearcs. *Tectonics*, 12(1):123–144, Feb. 1993. doi: 10.1029/92tc00618.

Carbotte, S., Han, S., and Boston, B. Cascadia seismic imaging experiment—CASIE21 MGL2104. Cruise report, 2021. doi: 10.26022/IEDA/330904.

Carbotte, S., Han, S., Boston, B., and Canales, J. Processed pre-stack depth-migrated seismic reflection data from the 2021 CASIE21 multi-channel seismic survey (MGL2104) [dataset], 2023. doi: 10.26022/IEDA/331274.

Carbotte, S. M., Boston, B., Han, S., Shuck, B., Beeson, J., Canales, J. P., Tobin, H., Miller, N., Nedimovic, M., Tréhu, A., Lee, M., Lucas, M., Jian, H., Jiang, D., Moser, L., Anderson, C., Judd, D., Fernandez, J., Campbell, C., Goswami, A., and Gahlawat, R. Subducting plate structure and megathrust morphology from deep seismic imaging linked to earthquake rupture segmentation at Cascadia. *Science Advances*, 10(23), June 2024. doi: 10.1126/sciadv.adl3198.

Chaytor, J. D., Goldfinger, C., Dziak, R. P., and Fox, C. G. Active deformation of the Gorda plate: Constraining deformation models with new geophysical data. *Geology*, 32(4):353, 2004. doi: 10.1130/g20178.2.

Clark, J., Mitrovica, J. X., and Alder, J. Coastal paleogeography of the California–Oregon–Washington and Bering Sea continental shelves during the latest Pleistocene and Holocene: implications for the archaeological record. *Journal of Archaeological Science*, 52:12–23, Dec. 2014. doi: 10.1016/j.jas.2014.07.030.

Collot, J., Agudelo, W., Ribodetti, A., and Marcaillou, B. Origin of a crustal splay fault and its relation to the seismogenic zone and underplating at the erosional north Ecuador–south Colombia oceanic margin. *Journal of Geophysical Research: Solid Earth*, 113(B12), Dec. 2008. doi: 10.1029/2008jb005691.

Cook, B. J., Henstock, T. J., McNeill, L. C., and Bull, J. M. Controls on spatial and temporal evolution of prism faulting and relationships to plate boundary slip offshore north-central Sumatra. *Journal of Geophysical Research: Solid Earth*, 119(7):5594–5612, July 2014. doi: 10.1002/2013jb010834.

Cowan, D. S. Structural styles in Mesozoic and Cenozoic mélanges in the western Cordillera of North America. *Geological Society of America Bulletin*, 96(4):451, 1985. doi: 10.1130/0016-7606(1985)96<451:ssimac>2.0.co;2.

Cummins, P. R. and Kaneda, Y. Possible splay fault slip during the 1946 Nankai earthquake. *Geophysical Research Letters*, 27(17): 2725–2728, Sept. 2000. doi: 10.1029/1999gl011139.

Dahlen, F. A. Critical taper model of fold-and-thrust belts and accretionary wedges. *Annual Review of Earth and Planetary Sciences*, 18(1):55–99, May 1990. doi: 10.1146/annurev.ea.18.050190.000415.

Dartnell, P., Conrad, J. E., Watt, J. T., and Hill, J. C. Composite multibeam bathymetry surface and data sources of the southern Cascadia Margin offshore Oregon and northern California [dataset], 2021. doi: 10.5066/P9C5DBMR.

Dartnell, P., Watt, J. T., Hill, J. C., and Conrad, J. E. Composite multibeam bathymetry surface and data sources of the central Cascadia Margin offshore Oregon [dataset], 2023. doi: 10.5066/P9PERGFK.

Davis, E. E. and Hyndman, R. D. Accretion and recent deformation of sediments along the northern Cascadia subduction zone. *Geological Society of America Bulletin*, 101(11):1465–1480, Nov. 1989. doi: 10.1130/0016-7606(1989)101<1465:aardos>2.3.co;2.

Dolcimascolo, A., Eungard, D., Allen, C., LeVeque, R., Adams, L., Arcas, D., Titov, V., González, F., Moore, C., and Garrison-Laney, C. Tsunami Hazard Maps of the Puget Sound and Adjacent Waters–Model Results from a 2,500-year Magnitude 9.0 Cascadia Subduction Zone Earthquake Scenario. Washington Geological Survey Map Series 2021-01, 16 sheets, scale 1:48,000, 2022.

Dominguez, S., Malavieille, J., and Lallemand, S. E. Deformation of accretionary wedges in response to seamount subduction: Insights from sandbox experiments. *Tectonics*, 19(1):182–196, Feb. 2000. doi: 10.1029/1999tc900055.

Flinch, J., Amaral, J., Doulcet, A., Mouly, B., Osorio, C., and Pince, J. Structure Of The Offshore Sinu Accretionary Wedge. In *8th Simposio Bolivariano - Exploracion Petrolera en las Cuencas Subandinas*. European Association of Geoscientists and Engineers, 2003. doi: 10.3997/2214-4609-pdb.33.paper8.

Flueh, E. R., Fisher, M. A., Bialas, J., Childs, J. R., Klaeschen, D., Kukowski, N., Parsons, T., Scholl, D. W., ten Brink, U., Tréhu, A. M., and Vidal, N. New seismic images of the Cascadia subduction zone from cruise SO108 — ORWELL. *Tectonophysics*, 293 (1–2):69–84, July 1998. doi: 10.1016/s0040-1951(98)00091-2.

Gao, D., Wang, K., Insua, T. L., Sypus, M., Riedel, M., and Sun, T. Defining megathrust tsunami source scenarios for northernmost Cascadia. *Natural Hazards*, 94(1):445–469, July 2018. doi: 10.1007/s11069-018-3397-6.

Geist, E. and Yoshioka, S. Source parameters controlling the generation and propagation of potential local tsunamis along the Cascadia margin. *Natural Hazards*, 13(2):151–177, Mar. 1996. doi: 10.1007/bf00138481.

Goldfinger, C. *Active deformation of the Cascadia forearc: Implications for great earthquake potential in Oregon and Washington*. PhD thesis, Oregon State University, 1994. https://ir.library.oregonstate.edu/concern/graduate_thesis_or_dissertations/w37639397.

Goldfinger, C., Kulm, L. D., Yeats, R. S., McNeill, L., and Hummon, C. Oblique strike-slip faulting of the central Cascadia submarine forearc. *Journal of Geophysical Research: Solid Earth*, 102(B4): 8217–8243, Apr. 1997. doi: 10.1029/96jb02655.

Haeussler, P. J., Armstrong, P. A., Liberty, L. M., Ferguson, K. M., Finn, S. P., Arkle, J. C., and Pratt, T. L. Focused exhumation along megathrust splay faults in Prince William Sound, Alaska. *Quaternary Science Reviews*, 113:8–22, Apr. 2015. doi: 10.1016/j.quascirev.2014.10.013.

Han, S., Carbotte, S. M., Canales, J. P., Nedimović, M. R., and Carton, H. Along-Trench Structural Variations of the Subducting Juan de Fuca Plate From Multichannel Seismic Reflection Imaging. *Journal of Geophysical Research: Solid Earth*, 123(4): 3122–3146, Apr. 2018. doi: 10.1002/2017jb015059.

Harding, T. and Lowell, J. Structural Styles, Their Plate-Tectonic Habitats, and Hydrocarbon Traps in Petroleum Provinces. *AAPG Bulletin*, 63(7):1016–1058, 1979.

Hill, J. C., Watt, J. T., and Brothers, D. S. Mass wasting along the Cascadia subduction zone: Implications for abyssal turbidite sources and the earthquake record. *Earth and Planetary Science Letters*, 597:117797, Nov. 2022. doi: 10.1016/j.epsl.2022.117797.

Hutchinson, J., Kao, H., Riedel, M., Obana, K., Wang, K., Kodaira, S., Takahashi, T., and Yamamoto, Y. Tectonic evolution of the Nootka fault zone and deformation of the shallow subducted Explorer plate in northern Cascadia as revealed by earthquake distributions and seismic tomography. *Scientific Reports*, 13(1), May 2023. doi: 10.1038/s41598-023-33310-z.

Hyndman, R. D., Yorath, C. J., Clowes, R. M., and Davis, E. E. The northern Cascadia subduction zone at Vancouver Island: seismic structure and tectonic history. *Canadian Journal of Earth Sciences*, 27(3):313–329, Mar. 1990. doi: 10.1139/e90-030.

Jurado, M. J. and Comas, M. C. Well log interpretation and seismic character of the cenozoic sequence in the northern Alboran Sea. *Geo-Marine Letters*, 12(2–3):129–136, June 1992. doi: 10.1007/bf02084923.

Klotsko, S., Skakun, M., Maloney, J., Gusick, A., Davis, L., Nyers, A., and Ball, D. Geologic controls on paleodrainage incision and morphology during sea level lowstands on the Cascadia shelf in Oregon, USA. *Marine Geology*, 434:106444, Apr. 2021. doi: 10.1016/j.margeo.2021.106444.

Kopp, H. The control of subduction zone structural complexity and geometry on margin segmentation and seismicity. *Tectonophysics*, 589:1–16, Mar. 2013. doi: 10.1016/j.tecto.2012.12.037.

Kopp, H. and Kukowski, N. Backstop geometry and accretionary mechanics of the Sunda margin. *Tectonics*, 22(6), Dec. 2003. doi: 10.1029/2002tc001420.

La Selle, S. M., Nelson, A. R., Witter, R. C., Jaffe, B. E., Gelfenbaum, G., and Padgett, J. S. Testing Megathrust Rupture Models Using Tsunami Deposits. *Journal of Geophysical Research: Earth Surface*, 129(5), May 2024. doi: 10.1029/2023jf007444.

Ledeczi, A., Lucas, M., Tobin, H., Watt, J., and Miller, N. Late Quaternary Surface Displacements on Accretionary Wedge Splay Faults in the Cascadia Subduction Zone: Implications for Megathrust Rupture. *Seismica*, 2(4), Apr. 2024. doi: 10.26443/seismica.v2i4.1158.

Lee, C.-J. Tsunami Inundation Modeling of Sequim Bay Area, Washington, USA from a Mw 9.0 Cascadia Subduction Zone Earthquake. Master's thesis, University of Washington, 2017. http://hdl.handle.net/1773/44994.

Lee, M. W., Hutchinson, D. R., Agena, W. F., Dillon, W. P., Miller, J. J., and Swift, B. A. Seismic character of gas hydrates on the Southeastern U.S. continental margin. *Marine Geophysical Researches*, 16(3):163–184, June 1994. doi: 10.1007/bf01237512.

Li, F., Lyu, B., Qi, J., Verma, S., and Zhang, B. Seismic Coherence for Discontinuity Interpretation. *Surveys in Geophysics*, 42(6): 1229–1280, Nov. 2021. doi: 10.1007/s10712-021-09670-4.

Liberty, L. M., Finn, S. P., Haeussler, P. J., Pratt, T. L., and Peterson, A. Megathrust splay faults at the focus of the Prince William Sound asperity, Alaska. *Journal of Geophysical Research: Solid Earth*, 118(10):5428–5441, Oct. 2013. doi: 10.1002/jgrb.50372.

Lotto, G. C., Jeppson, T. N., and Dunham, E. M. Fully Coupled Simulations of Megathrust Earthquakes and Tsunamis in the Japan Trench, Nankai Trough, and Cascadia Subduction Zone. *Pure and Applied Geophysics*, 176(9):4009–4041, Sept. 2018. doi: 10.1007/s00024-018-1990-y.

Løseth, H., Gading, M., and Wensaas, L. Hydrocarbon leakage interpreted on seismic data. *Marine and Petroleum Geology*, 26(7): 1304–1319, Aug. 2009. doi: 10.1016/j.marpetgeo.2008.09.008.

Mann, D. M. and Snavely, P. D. Multichannel seismic-reflection profiles collected in 1977 in the eastern Pacific Ocean off of the Washington/Oregon coast. Open-File Report 2331-1258, US Geological Survey, 1984. doi: 10.3133/ofr845.

Mannu, U., Ueda, K., Willett, S. D., Gerya, T. V., and Strasser, M. Impact of sedimentation on evolution of accretionary wedges: Insights from high-resolution thermomechanical modeling: Sedimentation in Accretionary Wedges. *Tectonics*, 35(12): 2828–2846, Dec. 2016. doi: 10.1002/2016tc004239.

McArthur, A. D., Bailleul, J., Mahieux, G., Claussmann, B., Wunderlich, A., and McCaffrey, W. D. Deformation–sedimentation feedback and the development of anomalously thick aggradational turbidite lobes: Outcrop and subsurface examples from the Hikurangi Margin, New Zealand. *Journal of Sedimentary Research*, 91(4):362–389, Apr. 2021. doi: 10.2110/jsr.2020.013.

McCaffrey, R., Qamar, A. I., King, R. W., Wells, R., Khazaradze, G., Williams, C. A., Stevens, C. W., Vollick, J. J., and Zwick, P. C. Fault locking, block rotation and crustal deformation in the Pacific Northwest. *Geophysical Journal International*, 169(3): 1315–1340, June 2007. doi: 10.1111/j.1365-246x.2007.03371.x.

McNeill, L. C. and Henstock, T. J. Forearc structure and morphology along the Sumatra-Andaman subduction zone. *Tectonics*, 33(2): 112–134, Feb. 2014. doi: 10.1002/2012tc003264.

McNeill, L. C., Piper, K. A., Goldfinger, C., Kulm, L. D., and Yeats, R. S. Listric normal faulting on the Cascadia continental margin. *Journal of Geophysical Research: Solid Earth*, 102(B6): 12123–12138, June 1997. doi: 10.1029/97jb00728.

McNeill, L. C., Goldfinger, C., Kulm, L. D., and Yeats, R. S. Tectonics of the Neogene Cascadia forearc basin: Investigations of a deformed late Miocene unconformity. *Geological Society of America Bulletin*, 112(8):1209–1224, Aug. 2000. doi: 10.1130/0016-7606(2000)112<1209:totncf>2.0.co;2.

Moore, G. F., Bangs, N. L., Taira, A., Kuramoto, S., Pangborn, E., and Tobin, H. J. Three-Dimensional Splay Fault Geometry and Implications for Tsunami Generation. *Science*, 318(5853):1128–1131, Nov. 2007. doi: 10.1126/science.1147195.

Moore, J. C. and Vrolijk, P. Fluids in accretionary prisms. *Reviews of Geophysics*, 30(2):113–135, May 1992. doi: 10.1029/92rg00201.

Moore, J. C., Cowan, D. S., and Karig, D. E. Structural styles and deformation fabrics of accretionary complexes. *Geology*, 13(1): 77, 1985. doi: 10.1130/0091-7613(1985)13<77:ssadfo>2.0.co;2.

Morkner, P. Validation of Predicted Tsunami Inundation for the Inland Coast of the Salish Sea Associated with Cascadia Subduction Zone Earthquakes. Master's thesis, Western Washington University, 2019. https://cedar.wwu.edu/wwuet/895.

Nedimović, M. R., Bohnenstiehl, D. R., Carbotte, S. M., Pablo Canales, J., and Dziak, R. P. Faulting and hydration of the Juan de Fuca plate system. *Earth and Planetary Science Letters*, 284(1–2):94–102, June 2009. doi: 10.1016/j.epsl.2009.04.013.

Noda, A., Koge, H., Yamada, Y., Miyakawa, A., and Ashi, J. Forearc Basin Stratigraphy Resulting From Syntectonic Sedimentation During Accretionary Wedge Growth: Insights From Sandbox Analog Experiments. *Tectonics*, 39(3), Mar. 2020. doi: 10.1029/2019tc006033.

Palmer, S. and Lingley, W. An Assessment Of The Oil And Gas Potential Of The Washington Outer Continental Shelf. Technical Report WASHU-T-89-001, Washington State Offshore Oil and Gas, Washington Sea Grant, 1989. https://repository.library.noaa.gov/view/noaa/36024/noaa_36024_DS1.pdf.

Park, J.-O., Tsuru, T., Kodaira, S., Cummins, P. R., and Kaneda, Y. Splay Fault Branching Along the Nankai Subduction Zone. *Science*, 297(5584):1157–1160, Aug. 2002. doi: 10.1126/science.1074111.

Plafker, G. Tectonic Deformation Associated with the 1964 Alaska Earthquake. *Science*, 148(3678):1675–1687, June 1965. doi: 10.1126/science.148.3678.1675.

Plafker, G. Tectonics of the March 27, 1964, Alaska earthquake. Open-file report 2330-7102, US Geological Survey, 1969. doi: 10.3133/pp543i.

Priest, G. R., Goldfinger, C., Wang, K., Witter, R. C., Zhang, Y., and Baptista, A. M. Confidence levels for tsunami-inundation limits in northern Oregon inferred from a 10,000-year history of great earthquakes at the Cascadia subduction zone. *Natural Hazards*, 54(1):27–73, Sept. 2009. doi: 10.1007/s11069-009-9453-5.

Ren, Y., Lange, D., and Grevemeyer, I. Seismotectonics of the Blanco Transform Fault System, Northeast Pacific: Evidence for an Immature Plate Boundary. *Journal of Geophysical Research: Solid Earth*, 128(3), Mar. 2023. doi: 10.1029/2022jb026045.

Richter, P. P., Ring, U., Willner, A. P., and Leiss, B. Structural contacts in subduction complexes and their tectonic significance: the Late Palaeozoic coastal accretionary wedge of central Chile. *Journal of the Geological Society*, 164(1):203–214, Jan. 2007. doi: 10.1144/0016-76492005-181.

Rohr, K. M. M., Furlong, K. P., and Riedel, M. Initiation of Strike-Slip Faults, Serpentinization, and Methane: The Nootka Fault Zone, the Juan de Fuca-Explorer Plate Boundary. *Geochemistry, Geophysics, Geosystems*, 19(11):4290–4312, Nov. 2018. doi: 10.1029/2018gc007851.

Ryan, W. B. F., Carbotte, S. M., Coplan, J. O., O'Hara, S., Melkonian, A., Arko, R., Weissel, R. A., Ferrini, V., Goodwillie, A., Nitsche, F., Bonczkowski, J., and Zemsky, R. Global Multi-Resolution Topography synthesis. *Geochemistry, Geophysics, Geosystems*, 10 (3), Mar. 2009. doi: 10.1029/2008gc002332.

Shuck, B., Boston, B., Carbotte, S., Han, S., Becel, A., Gurun, P., Beeson, J., Canales, J., Miller, N., and Tobin, H. The Role of the Nootka Fault Zone in the Ongoing Capture of the Explorer Microplate and Cessation of Subduction along Northern Cascadia. *AGU Fall Meeting*, T51A–02, 2023.

Sibuet, J., Rangin, C., LePichon, X., Singh, S., Cattaneo, A., Graindorge, D., Klingelhoefer, F., Lin, J., Malod, J., and Maury, T. 26th December 2004 great Sumatra–Andaman earthquake: Co-seismic and post-seismic motions in northern Sumatra. *Earth and Planetary Science Letters*, 263(1–2):88–103, Nov. 2007. doi: 10.1016/j.epsl.2007.09.005.

Silver, E. A. Pleistocene tectonic accretion of the continental slope off Washington. *Marine Geology*, 13(4):239–249, Nov. 1972. doi: 10.1016/0025-3227(72)90053-9.

Silver, E. A., Ellis, M. J., Breen, N. A., and Shipley, T. H. Comments on the growth of accretionary wedges. *Geology*, 13(1):6, 1985. doi: 10.1130/0091-7613(1985)13<6:cotgoa>2.0.co;2.

Simpson, G. D. Formation of accretionary prisms influenced by sediment subduction and supplied by sediments from adjacent continents. *Geology*, 38(2):131–134, Feb. 2010. doi: 10.1130/g30461.1.

Snavely, Jr., P. *Geology and Resource Potential of the Western North America and Adjacent Ocean Basins*, volume 6, chapter Tertiary Geologic Framework, Neotectonics, and Petroleum Potential of the Oregon-Washington Continental Margin. Circum-Pacific Council for Energy and Mineral Resources, 1987.

Strasser, M., Moore, G. F., Kimura, G., Kitamura, Y., Kopf, A. J., Lallemant, S., Park, J.-O., Screaton, E. J., Su, X., Underwood, M. B., and Zhao, X. Origin and evolution of a splay fault in the Nankai accretionary wedge. *Nature Geoscience*, 2(9):648–652, Aug. 2009. doi: 10.1038/ngeo609.

Sypus, M. Models of tsunamigenic earthquake rupture along the west coast of North America. Master's thesis, University of Victoria, 2019.

Tobin, H. J. and Kinoshita, M. NanTroSEIZE: The IODP Nankai Trough Seismogenic Zone Experiment. *Scientific Drilling*, 2: 23–27, Mar. 2006. doi: 10.5194/sd-2-23-2006.

Underwood, M. B. Strike-parallel variations in clay minerals and fault vergence in the Cascadia subduction zone. *Geology*, 30(2):155, 2002. doi: 10.1130/0091-7613(2002)030<0155:spvicm>2.0.co;2.

Walton, M. A., Staisch, L. M., Dura, T., Pearl, J. K., Sherrod, B., Gomberg, J., Engelhart, S., Tréhu, A., Watt, J., Perkins, J., Witter, R. C., Bartlow, N., Goldfinger, C., Kelsey, H., Morey, A. E., Sahakian, V. J., Tobin, H., Wang, K., Wells, R., and Wirth, E. Toward an Integrative Geological and Geophysical View of Cascadia Subduction Zone Earthquakes. *Annual Review of Earth and Planetary Sciences*, 49(1):367–398, May 2021. doi: 10.1146/annurev-earth-071620-065605.

Wang, K. and Tréhu, A. M. Invited review paper: Some outstanding issues in the study of great megathrust earthquakes—The Cascadia example. *Journal of Geodynamics*, 98:1–18, Aug. 2016. doi: 10.1016/j.jog.2016.03.010.

Watt, J. T. and Brothers, D. S. Systematic characterization of morphotectonic variability along the Cascadia convergent margin: Implications for shallow megathrust behavior and tsunami hazards. *Geosphere*, 17(1):95–117, Nov. 2020. doi: 10.1130/ges02178.1.

Webb, S. *Interaction of structure and physical properties in accretionary wedges: Examples from the Cascadia and Nankai Trough subduction zones*. PhD thesis, University of Wisconsin, Madison, 2017.

Wells, R. E., Weaver, C. S., and Blakely, R. J. Fore-arc migration in Cascadia and its neotectonic significance. *Geology*, 26(8):759, 1998. doi: 10.1130/0091-7613(1998)026<0759:famica>2.3.co;2.

Wendt, J., Oglesby, D. D., and Geist, E. L. Tsunamis and splay fault dynamics. *Geophysical Research Letters*, 36(15), Aug. 2009. doi: 10.1029/2009gl038295.

Wilson, D. S. *The Cascadia subduction zone and related subduction systems - seismic structure, intraslab earthquakes and processes, and earthquake hazards*, chapter The Juan de Fuca plate and slab: isochron structure and Cenozoic plate motions. Natural Resources Canada, 2002. doi: 10.4095/222387. Open File 4350 9-12.

Witter, R. C., Zhang, Y. J., Wang, K., Priest, G. R., Goldfinger, C., Stimely, L., English, J. T., and Ferro, P. A. Simulated tsunami inundation for a range of Cascadia megathrust earthquake scenarios at Bandon, Oregon, USA. *Geosphere*, 9(6):1783–1803, Dec. 2013. doi: 10.1130/ges00899.1.